Multimodal Transportation 3 (2024) 100165

Contents lists available at ScienceDirect

Multimodal Transportation

journal homepage: www.elsevier.com/locate/multra

Full Length Article

# Co-optimizing electric bus dispatching and charging considering limited resources and battery degradation

Chenming Niu[a,b], Qiuzi Chen[a,c], Ran Tu[a,c,*], Di Huang[a], Yujian Ye[d,e]

[a] School of Transportation, Southeast University, China
[b] Department of Civil and Environmental Engineering, University of California, Berkeley, USA
[c] Key Laboratory of Transport Industry of Comprehensive Transportation Theory (Nanjing Modern Multimodal Transportation Laboratory), Ministry of Transport, China
[d] School of Electrical Engineering, Southeast University, China
[e] State Key Laboratory of Power System Operation and Control, Department of Electrical Engineering, Tsinghua University, China

ARTICLE INFO

*Keywords:*
Bus-to-trip assignment
Partial charging schedule
Fleet composition
Battery degradation
Energy consumption uncertainty

ABSTRACT

This paper aims to formulate a mathematical model for a multi-type electric bus scheduling problem to determine the optimal fleet composition, bus-to-trip assignment, and partial charging schedule, where the battery degradation, nonlinear charging, and the constraint of charging station capacity are considered. A time-expanded network is proposed to represent the bus-to-trip assignment and partial charging. An adaptive large neighborhood search algorithm is designed to solve the problem. Using a multi-line bus network in Nanjing as the case, empirical operational data is used to generate monthly timetable samples to simulate the uncertainty of trip travel time and energy consumption. The result shows that the charging station capacity can be reduced from 20 (real-world case) to 12, considering the cost-effectiveness and robustness of the bus system. The result of this study also provides suggestions on the charging duration choices and the starting state-of-charge for different periods of the day. In peak and off-peak hours, 20-30-minute charging is recommended for electric buses with state-of-charge lower than 30 %, and 10-minute charging is more recommended when the state-of-charge of the electric bus is between 30 % and 70 %.

## 1. Introduction

### 1.1. Background and motivation

Electric buses (EBs) have been proven to be more sustainable and cost-competitive compared to internal combustion engine buses (ICEBs) (An, 2020; Dunn et al., 2015; Pelletier et al., 2019; Wu et al., 2018). Public transportation electrification has been serving as an effective method to tackle the challenge of urban greenhouse gas emissions (Bao et al., 2023; Chen et al., 2023). In recent years, policies and plans have been launched around the globe to facilitate the development of EBs (Land Transport Authority, 2022; The State Council of People's Republic of China, 2021; United States Department of Transportation, 2021).

Despite the environmental benefits of EBs, challenges such as high investment costs and limited driving range persist in the planning and operational stages of the EB system, hindering the large-scale adoption of EBs (Chen et al., 2023; Quarles et al., 2020). The planning and operation of EB are inseparable and require systematic optimization. In the planning stage, fleet composition and

* Corresponding author.
*E-mail addresses:* chenming_niu@berkeley.edu (C. Niu), qiuzi.chen@outlook.com (Q. Chen), turancoolgal@seu.edu.cn (R. Tu), dihuang@seu.edu.cn (D. Huang), yeyujian@seu.edu.cn (Y. Ye).

https://doi.org/10.1016/j.multra.2024.100165
Received 17 December 2023; Received in revised form 14 April 2024; Accepted 16 May 2024

the number of chargers at the depot (or charging station) significantly influence EB charging schedule in the operational stage. EBs with smaller battery capacity have lower prices but require more charging resources with more complex charging schedules, while EBs with larger battery capacity have a longer driving range but have higher energy consumption rates and purchase cost (Liu and Song, 2017). Therefore, a mixed EB fleet consisting of multiple bus types should be optimized to reduce initial purchase costs while maintaining daily service. In addition, to increase revenue and public convenience, some cities (such as Shenzhen) have piloted opening EB chargers to social vehicles, such as taxis and e-hailing vehicles (Shenzhen Press Group Greater Bay Area News, 2023). However, this poses another issue to EB scheduling. The opening of charging stations reduces available chargers for EBs during operation, and thus charging opportunities for EBs are restricted. Given the aforementioned limitations, optimization of mixed fleet and charging schedule can make better use of intervals between service trips to charge the EBs. This enables an optimized charging schedule to reduce the fleet size and the need for EBs with large battery capacity (Bao et al., 2023; Chen et al., 2023; Liu et al., 2021; Liu and Song, 2017).

In the operational stage, the scheduling of EBs needs to consider both the service constraint (each service be fulfilled) and the battery energy constraint (battery energy within a safe range). Moreover, the charging station capacity constraint is not negligible due to the long charging duration. In addition, the battery capacity is degraded with respect to the number of charge-and-discharge cycles and the depth of charge-and-discharge (Pelletier et al., 2017). Therefore, improper charging schedules may lead to shorter battery life (Lam and Bauer, 2013; Zhang et al., 2021; Zhou et al., 2022). The end of life (EoL) of a battery is defined as the usable lifecycle of the battery (Zhang et al., 2019). According to Zhou et al. (2022), the typical EoL of current batteries is less than three years. The degrading health of the battery significantly elevates the maintenance cost of EBs. This significantly elevates the maintenance cost of EBs. From the perspective of daily operation, the cost of battery degradation is about 2.7 times higher than EB daily charging cost under specific conditions (Zhou et al., 2022). Therefore, it's important to incorporate the battery degradation effect into the optimization model. Besides, the trip travel time and energy consumption of EBs during operation are not deterministic and are affected by several factors, such as traffic conditions, driving behaviors, and weather conditions (Bie et al., 2021). The stochasticity of trips can raise concerns about the robustness of resource allocation and intensify driving range anxiety, resulting in the purchase of extra EBs.

To tackle the aforementioned challenges, it is crucial to develop an optimization framework that can provide robust cost-effective resource allocation and operation schedule while satisfying daily service and charging demand. Distinct from prior research, this study establishes a mixed integer programming (MIP) model for the EB scheduling problem (EBSP) based on a novel time-expanded network. The design of the time-expanded network allows concurrent planning and operation decisions for fleet composition, bus-to-trip schedule, and charging schedule. Nonlinear charging and battery degradation are considered to realistically simulate the charging process in real-world scenarios. Variations in trip travel time and energy consumption are captured through distribution simulation (DS). A real-world case study is conducted to provide cost-effective and robust suggestions for EB resource allocation and operation schedule. Note that the robustness in this study refers to robust resource and charging decisions that work for the EB system with uncertain energy consumption. It is within the frame of strategy robustness instead of the formulation of robust optimization. Similar definitions can be found in existing research, such as Tu et al. (2020) and Wang et al. (2020).

### *1.2. Literature review*

The EBSP can optimize both the charging schedule and the bus-to-trip assignment schedule for a single-type or multi-type EB fleet. However, researchers usually explored these two correlated topics separately. The first topic, the EB charging scheduling problem (EBCSP), determines the charging start time and charging duration. In the studies of EBCSP, the operation schedule of EB, namely the bus-to-trip assignment schedule, is predetermined, and the charging schedule of EBs is subject to the time windows of the operation schedule. The second topic, the bus-to-trip scheduling problem (BTSP), determines the most effective way to schedule EBs to serve pre-compiled trips according to assumptions of fixed charging duration or fully-charged policy. The BTSP is consistent with the EBSP except for the charging assumption, but the EBCSP is distinct from the EBSP in that the EBCSP does not optimize the bus-to-trip assignment and the fleet composition.

The research on EBCSP assumes that all trips on the timetable have been pre-assigned to EBs and sufficient charging time is allowed between consecutive trips to optimize the charging schedule of EBs (Bao et al., 2023; Liu et al., 2021). In terms of influencing factors and constraints, vehicle energy consumption (Qin et al., 2016), charging power (He et al., 2022; Leou and Hung, 2017; Liu et al., 2021), and the number of available chargers (Leou and Hung, 2017; Liu et al., 2021) are the major elements when optimizing the charging schedule. For example, Liu et al. (2021) proposed a MIP model to optimize the charging schedule and charging power for large-scale EB networks that cover the limited charging resources in the charging station and the time-of-use (TOU) electricity price.

From the perspective of the modeling framework, with the assumption of the predetermined operation schedule, continuous variables that directly determines the charging start time and duration (He et al., 2020; Wen et al., 2016), and binary variables that choose discrete time slots (Bao et al., 2023; Liu et al., 2021; Manzolli et al., 2022; Wang et al., 2017) are the most used methods to formulate the EBCSP. Both modeling frameworks can be solved in a reasonable timeframe due to fewer variables than the EBSP. However, the assumption of EBCSP that trips are preassigned to EBs results in a circumstance where many EBs are idle at the depot instead of getting charged or executing tasks (Zhou et al., 2022). In this case, inefficient EB usage is demonstrated.

Contrary to EBCSP, the EBSP focuses on assigning single-type or multi-type EBs to serve trips by simplifying charging behavior. Given a timetable including start time, travel time, the energy consumption of trips, and the location of charging stations, the EBSP assigns EBs to fulfill each trip exactly once and get charged at the charging station to ensure that the battery state-of-charging (SoC)

of each EB is within safe range at any time during operation. The EBSP includes two assumptions on the charging behavior: the fully charged assumption and the fixed duration assumption.

a. The fully charged assumption stipulates that EBs must be charged to full capacity once they start charging, and the charging duration can be obtained from the inverse function of the charging function (Li, 2014; Rogge et al., 2018; Zhang et al., 2021). For example, Li investigated the EBSP considering fully fast charging or battery swapping techniques. The charging duration is assumed to be discrete, composed of several 10-minute intervals (Li, 2014).
b. The fixed charging duration assumption specifies that the duration of each charging session is fixed (Chen et al., 2023; Li et al., 2019; Tang et al., 2019). Tang et al. regarded the charging duration as a fixed time of 30 minutes and adopted a discrete time-expanded graph to illustrate the EBSP (Tang et al., 2019). Similarly, Li et al. specified that the energy gained from each refueling or charging event is fixed and established a time-space-energy network to represent the EBSP considering the charging station location (Li et al., 2019).

Although these assumptions of charging events can simplify the EBSP and effectively reduce the number of variables, they cannot reflect the reality that EBs during operation can get charged at any time for any duration within the time and battery capacity constraints. Therefore, the combination of EBSP and partial-charging policy (variable charging start time and duration) is urged for a more practical solution (Jiang et al., 2021; Yıldırım and Yıldız, 2021; Zhou et al., 2022).

In the scenarios of both EBCSP and EBSP, there exist challenges of how to reasonably simulate the practical charging process. The nonlinear characteristic of the charging process is considered in many related studies (Zeng et al., 2022; Zhang et al., 2021; Zhou et al., 2022). In the charging process, when the SoC of an EB reaches a certain level, the SoC increases concavely with time instead of increasing linearly. Another important factor in the charging process is the battery degradation effect, which is related to the SoC before and after charging. Improper charging behavior may lead to additional battery degradation and thus increase the operational cost (Barré et al., 2013; Guo et al., 2022; Lam and Bauer, 2013). Besides, the charging schedule is significantly affected by the trip travel time and energy consumption. The stochasticity of travel time and energy consumption may not only impact the resource allocation of the EB system (including mixed fleet composition and charging station capacity) but also alter the battery degradation rate. Therefore, it is of utmost importance from the perspective of cost-effectiveness and resource robustness to incorporate both battery health and trip uncertainty in the optimization of EBSP. Although some research studied the EBSP considering battery degradation (Zhang et al., 2021; Zhou et al., 2022), our research takes the existing framework of EBSP a step further by integrating a time-expanded network to represent partial charging. In addition, we comprehensively consider a wide range of factors in EB charging and scheduling, including nonlinear charging, battery degradation, charging station capacity, battery capacity, and uncertainty of trip energy consumption.

### *1.3. Contributions*

To address research gaps in the optimization of EBSP, our paper introduces a new model framework for EBSP and partial charging behavior. The comparison between the state-of-art studies on EBSP and our study is presented in Table 1, and the major contributions of this study can be revealed threefold:

(1) This model framework covers the partial charging behavior (variable charging start time and charging duration), nonlinear charging characteristics, battery degradation effect, and charging station capacity, which is more in line with the actual operation situations.
(2) A unique time-expanded network to represent bus-to-trip assignments and partial charging is proposed, which approaches flexible charging slots. In addition, the discretization of the problem makes the model suitable for different types of solving algorithms, including, but not limited to, dynamic programming, adaptive large neighborhood search, and genetic algorithms.
(3) Sensitivity analysis on charging station capacity using empirical data offers decision suggestions concerning robust bus system resource allocation with consideration of uncertainties of travel time and energy consumption.

**Table 1**
Overview of literature on EBSP.

| Papers | Multi Bus Type | Charging station capacity | Nonlinear charging Function | Battery degradation effect | Partial charging | Algorithm |
|---|---|---|---|---|---|---|
| (Li, 2014) | | √ | | | | B&P |
| (Wen et al., 2016) | | | | | √ | ALNS |
| (Rogge et al., 2018) | √ | √ | | | | GA |
| (Li et al., 2019) | √ | √ | | | | CPLEX |
| (Tang et al., 2019) | | √ | | | | B&P |
| (Zhang et al., 2021) | | √ | √ | √ | | B&P |
| (Yıldırım and Yıldız, 2021) | √ | | √ | | | CG |
| (Alvo et al., 2021) | | √ | | | √ | Gurobi |
| (Zhou et al., 2022) | | | √ | √ | √ | CPLEX |
| (Zeng et al., 2022) | | | | √ | √ | CPLEX |
| (Chen et al., 2023) | √ | √ | √ | | | ALNS |
| This paper | √ | √ | √ | √ | √ | ALNS |

### 1.4. Paper organization

The rest of this paper is organized as follows: Section 2 mathematically formulates a MIP model for EBSP considering partial charging policy, battery degradation and nonlinear charging. Section 3 introduces the ALNS algorithm adopted for solving the EBSP. Case studies are conducted and the results are presented in Section 4. Section 5 concludes the study.

## 2. EBSP formulation

In our study, a single-depot multi-line transit network is adopted to define the EBSP. EBs of multiple types are assigned to fulfill a sequence of round-trips of multiple bus lines. The depot in the transit network is equipped with adequate chargers for night charging and is regarded as the origin and destination of dispatching. EBs are allowed to get partially charged at the charging station during daily operation if there exist available chargers. All EBs are assumed to be fully charged at the depot after finishing one day's operation to ensure that they have sufficient energy for the next day. The formulation for EBSP proposed in this paper adopts the following assumptions:

- All EBs of multi-lines are charged at the same charging station during operation since the transit network is in single-depot mode.
- The charging duration is assumed to be integer multiples of a fixed time interval. For instance, if the time interval is set to be 10 minutes, the charging duration should be in the set $\{10,\ 20,\ 30, \ldots\}$.

To explicitly formulate the EBSP, the notations and time-expanded network are described in Section 2.1, the battery degradation model and nonlinear charging function are presented in Section 2.2 and 2.3, respectively, and the MIP model for EBSP is built in Section 2.4. The time-expanded network innovatively utilizes discrete variables to represent partial charging behavior, eliminating the need for continuous variables to denote the charging start time and duration. The discrete feature elevates the applicability of different solving algorithms for the problem since partial charging behavior is represented by a node in the network. For discussion convenience, the list of notations in the problem formulation is given in Table 2.

### 2.1. Notations and time-expanded network

The EBSP is formulated based on a time-expanded network (a directed graph) $G = (N, A)$, where $N$ and $A$ represent all nodes and arcs in the network, respectively. We define bus type set $K = \{1, 2, \ldots, |K|\}$, in which each bus type $k \in K$ corresponds to a battery capacity $E^k$ and $|K|$ represents the total number of bus types. $N = D \cup T \cup F \cup R$ represents all nodes in the network, where $D$ represents all virtual depot nodes, $T$ represents all trip nodes, $F$ represents all charging nodes, and $R$ represents all virtual charging nodes. For single-depot operation mode, $D = \{o, d\}$ includes virtual depot nodes $o$ and $d$ to denote the start and end of each EB's daily operation, respectively. The trip nodes set $T$ contains all the trips on the timetable required to be finished by EBs. For simplicity, we refer to the round-trip as one trip for short, because the bus returns back immediately after reaching the last station of the upward trip. For a trip or depot node $\in T \cup D$, the start time, travel time, and energy consumption are defined as $s_i$, $t_i$, and $e_i^k$ respectively. Note that travel time $t_d$ and energy consumption $e_d^k$ are set to zero, and start time $s_o$ and $s_d$ are set to be zero and large enough, respectively. Every trip node $i \in T$ corresponds to only one charging node $f_i \in F$, representing the charging event after finishing trip $i$.

To represent the partial charging policy, we discretize the time domain (5:00 – 24:00) into consecutive time nodes $N_t$ with an interval $\beta$. The virtual charging nodes set $R$ distinguishes from the charging nodes set $F$ in the sense that the virtual charging node is a dummy time-expanded node set that does not represent real charging events. For each virtual charging node $r \in R$, the charging start time and duration are defined as $s_r$ and $t_r$ respectively, where $s_r \in N_t$ and $t_r = m*\beta$. $m$ is an integer number constrained by the time that the EB with the largest battery capacity requires to get fully charged. For a time node $n_t \in N_t$, we define $u_{n_t r}$ to represent the occupation of virtual charging node $r \in R$ on the time node $n_t \in N_t$, where $u_{n_t r}$ equals one if the time node $n_t$ is after the start time and before the end time of virtual charging node $r$, and zero otherwise. The notation $u_{n_t r}$ is utilized for counting the EBs that are charging at any time node so that the constraint of charging station capacity can be easily formulated.

In the model, an arc $(i, j) \in A$ represents the connection, as well as the deadhead trip between node $i$ and node $j$. Four types of arcs are defined in each arc set $A$. First, deadhead trips from the depot to trip nodes, where $i \in \{o\}$, $j \in T$; second, deadhead trips returning to the depot from trip nodes, where $i \in T$, $j \in \{d\}$; third, deadhead trips between trip nodes, where $i,\ j \in T$, and $i \neq j$; lastly, deadhead trips between trip nodes and charging nodes, where $i \in T$ and $j \in F$, or $i \in F$ and $j \in T$. Furthermore, let $I$ be the set of indicators that represent directed connection from the charging node $f_i \in F$ to the virtual charging node $r \in R$ to pass charging start time $s_r$, charging duration $t_r$ and occupation $u_{n_t r}$ to the charging node.

For each arc $(i, j) \in A$, travel time $t_{ij}$ and energy consumption $e_{ij}^k$ are defined. In order to reduce the number of variables as much as possible, infeasible arcs and indicators through predetermined start time and travel time are excluded. From one trip node $i \in T$ to another trip node $j \in T$, arc $(i, j)$ is connected only if $s_i + t_i + t_{ij} \leq s_j$. Due to the correspondence between service trip nodes and charging nodes, only arc $(i, f_i)$ is connected for a trip node $i \in T$. From a charging node $f_i \in F$ to a trip node $j \in T$, arc $(f_i, j)$ is connected only if $s_i + t_i + t_{i,f_i} + t_{f_i,j} + 1 \times \beta \leq s_j$, where $1 \times \beta$ represents the minimum charging duration. From one charging node $f_i \in F$ to one virtual charging node $\in R$, indicator $(f_i,\ r)$ is connected only when $s_i + t_i + t_{if_i} \leq s_r$. A sample time-expanded network with 4 trips is presented in Fig. 1, illustrating the representation of the partial charging policy in this study. Virtual charging nodes $r_1$, $r_2$, $r_3$ and $r_4$ represent charging events with a charging duration of 10 minutes starting at 8:50, 9:00, 9:10, and 9:20, respectively. Similarly, $r_5$, $r_6$, $r_7$ and $r_8$ have the same starting times as $r_1$, $r_2$, $r_3$ and $r_4$, but their charging duration is extended to 20 mins. Each

**Table 2**
Notation.

| Notation | Description |
|---|---|
| Sets: | |
| $K$ | set of bus types |
| $D$ | set of virtual depot nodes, $D = \{o, d\}$ |
| $T$ | set of trip nodes |
| $F$ | set of charging nodes |
| $R$ | set of virtual charging nodes |
| $N_t$ | set of consecutive time nodes |
| $N$ | set of all nodes in the graph, $N = D \cup T \cup F \cup R$ |
| $A$ | set of arcs representing deadhead trips between nodes set $D \cup T \cup F$ |
| $I$ | set of indicators from charging node $f_i \in F$ to virtual charging node $r \in R$ |
| $\delta^+(i)$ | subset of arcs $A$ that start at node $i \in$ D ∪ T ∪ F |
| $\delta^-(i)$ | subset of arcs $A$ that end at node $i \in$ D ∪ T ∪ F |
| Parameters: | |
| $\|K\|$ | total number of bus types |
| $E^k$ | battery capacity of bus type $k \in K$ |
| $s_i$ | start time of trip node and depot node $i \in T \cup D$ |
| $t_i$ | travel time of trip node and depot node $i \in T \cup D$ |
| $e_i^k$ | energy consumption of trip and depot node $i \in T \cup D$ for bus type $k$ |
| $\beta$ | fixed time interval |
| $s_r$ | charging start time of virtual charging node $r \in R$ |
| $t_r$ | charging duration of virtual charging node $r \in R$ |
| $m$ | number of time intervals required for charging event |
| $u_{n_t r}$ | occupation of virtual charging node $r \in R$ on time node $n_t \in N_t$, set to one if $r$ is under charging at $n_t$ and zero otherwise |
| $t_{ij}$ | travel time of deadhead trip $(i, j) \in A$ |
| $e_{ij}^k$ | energy consumption of deadhead trip $(i, j) \in A$ for bus type $k \in K$ |
| $F_{DC}(\underline{SOC}^k, \overline{SOC^k})$ | average degradation cost function in a charge or discharge phase from lower bound $\underline{SOC}^k$ to upper bound $\overline{SOC^k}$ |
| $W(s, k)$ | wear density function of bus type $k$ at SoC $s$ |
| $BP^k$ | battery acquisition cost of bus type $k$ |
| $\mu$ | cycle efficiency |
| $a, b$ | battery dependent parameters |
| $H(t)$ | charging function in the constant current (CC) phase |
| $I_{cc}$ | constant charging current in the CC phase |
| $\overline{SOC}$ | SoC break point between the CC phase and the CV (constant voltage) phase |
| $\xi(t)$ | charging function in the CV phase |
| $F_{NC}(\underline{SOC}^k, t)$ | Piecewise nonlinear charging function of an initial SoC $\underline{SOC}^k$ and charging duration $t$ in both CC and CV phases |
| $H^{-1}, \xi^{-1}$ | inverse function of $H$ and $\xi$ |
| $c^k$ | daily depreciation cost of a single bus of type $k$ |
| $c_e$ | electricity cost per kWh |
| $c_t$ | labor cost per minute for service trips and deadhead arcs |
| $\sigma$ | battery safety level |
| $C$ | charging station capacity |
| Decision Variable | |
| $x_{ij}^k$ | binary variable, is set to one if an EB of type $k \in K$ is assigned to operate on arc or indicator $(i, j) \in A \cup I$, and zero otherwise. |
| Auxiliary Variables | |
| $y_i^k$ | continuous variable, denotes the remaining battery power of an EB of type $k \in K$ after completing node $i \in D \cup T \cup F$. |
| $s_{f_i}$ | continuous variable, denotes the start time of charging node $f_i \in F$. |
| $t_{f_i}$ | continuous variable, denotes the charging duration of charging node $f_i \in F$ |
| $u_{n_t f_i}$ | binary variable, is set to one if time node $n_t$ is after the start and before the end of charging node $f_i \in F$ |

virtual charging node $r \in R$ has a specific charging start time and duration, which can be passed to a charging node $f_i$ through the connection of indicator $(f_i, r)$. Taking the EB finishing $t_1$, $f_1$ and $t_4$ in Fig. 1 as an example, the connection between trip $t_1$ and $f_1$ represents that the EB decides to get charged after finishing trip $t_1$ and the directed connection of the indicator $(f_1, r_2)$ passes the charging start time (9:00), charging duration (10 minutes) and occupation on time nodes of virtual charging node $r_2$ to charging node $f_1$. Through this network, the mathematical model of EBSP does not require continuous decision variables to decide the charging start time and duration, which greatly simplifies the solving process.

### 2.2. Battery degradation model

The battery degradation cost is calculated using the model proposed by Han et al (Han et al., 2014), which has been applied in several previous studies to formulate the degradation effect (Zeng et al., 2022; Zhou et al., 2022). The degradation cost function

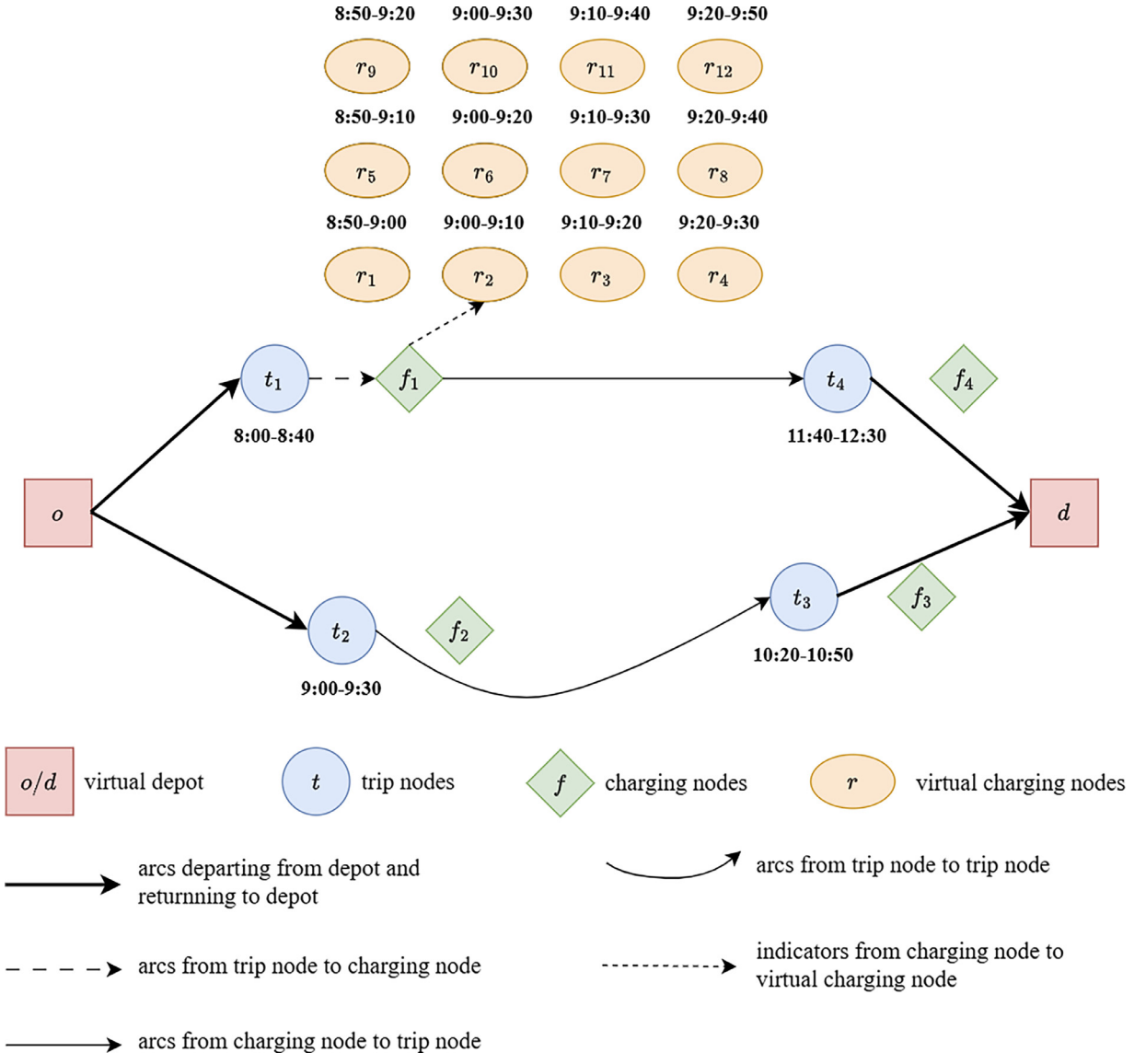


**Fig. 1.** Illustration of the time-expanded network.

($F_{DC}$) in a charge or discharge phase can be calculated as Eq. (1) and (2).

$$F_{DC}\left(\underline{SOC}^k,\ \overline{SOC^k}\right) = E^k \times \int_{\underline{SOC}^k}^{\overline{SOC^k}} W(s,k)ds \tag{1}$$

$$W(s,k) = \frac{BP^k}{2 \times E^k \times \mu^2} \times \frac{b(1-s)^{b-1}}{a} \tag{2}$$

where $\underline{SOC}^k$ represents the lower bound of the SoC of bus type $k$ for a charge or discharge phase; $\overline{SOC^k}$ represents the upper bound of the SoC of bus type k for a charge or discharge phase; $E^k$ is the battery capacity of bus type $k$; $W(s,k)$ is the wear density function of bus type $k$ at the SoC level s, which represents the unit degradation cost for a given SoC point; $BP^k$ is the battery acquisition cost of bus type $k$; $\mu$ is the cycle efficiency; $a$ and $b$ are the battery-dependent parameters. The sketched derivation of Eq. (1) and (2) from Han et al is explained in Appendix A (Han et al., 2014).

### 2.3. Nonlinear charging function

The battery of EB follows a nonlinear charging process, which can be divided into two phases: the constant current (CC) phase and the constant voltage (CV) phase. In the CC phase, namely the first phase, the charging current is constant and the SoC increases

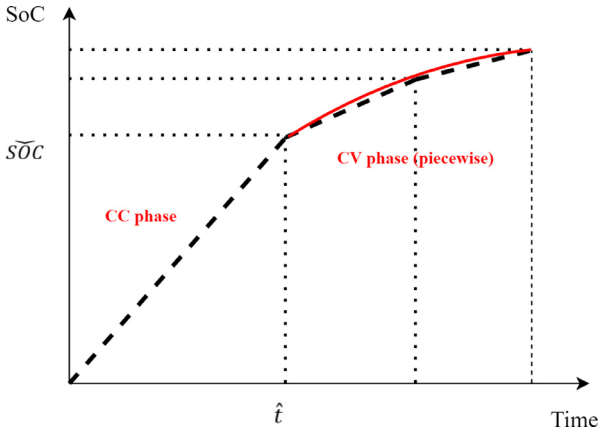


**Fig. 2.** Illustration of the nonlinear charging function.

over time linearly. The CC phase converts to the CV phase when the voltage reaches a maximum value. In the CV phase, namely the second phase, the charging voltage is constant and the current decreases exponentially. The SoC increases concavely with time in the CV phase (Montoya et al., 2017; Zhang et al., 2021). The time point $\hat{t}$ represents the break point between the CC phase and the CV phase. The charging function that calculates the charged amount in the first phase is denoted as $H$ presented in Eq. (3).

$$H(t) = I_{cc} \times t,\ t \in [0, \hat{t}] \tag{3}$$

where $I_{cc}$ represents the constant charging current. The charging function in the CV phase can be denoted as $\xi(t)$ for ease of presentation. A piecewise linear function is formulated to represent the nonlinear charging process of the CV phase (Montoya et al., 2017), as depicted in Fig. 2, where $\breve{SOC}$ represents the maximum SoC in the CC phase, the dash line is the piecewise function and the red curve is the actual charging process.

The charging function ($F_{NC}$) that calculates the SoC after the charging process maps the $\underline{SOC}^k$ and the charging duration $t$ onto the EB SoC level after charging. The nonlinear charging function $F_{NC}$ can be derived as Eq. (4).

$$F_{NC}\left(\underline{SOC}^k,\ t\right) = \begin{cases} \underline{SOC}^k + \frac{H(t)}{E^k}, & condition_1 \\ \min\left\{ \breve{SOC} + \frac{\xi\left(t + H^{-1}\left(\underline{SOC}^k\right) - \hat{t}\right)}{E^k}, 1 \right\}, & condition_2 \\ \min\left\{ \underline{SOC}^k + \frac{\xi\left(t + \xi^{-1}\left(\underline{SOC}^k - \breve{SOC}\right)\right)}{E^k}, 1 \right\}, & condition_3 \end{cases}$$

$$condition_1 : if\ \underline{SOC}^k \le \breve{SOC} \text{ and } \underline{SOC}^k + H(t) \le \breve{SOC}$$

$$condition_2 : if\ \underline{SOC}^k \le \breve{SOC} \text{ and } \underline{SOC}^k + H(t) > \breve{SOC}$$

$$condition_3 : if\ \underline{SOC}^k \ge \breve{SOC} \tag{4}$$

where $H^{-1}$ and $\xi^{-1}$ represent the inverse function of $H$ and $\xi$ respectively.

### 2.4. MIP model

A MIP model is formulated for the EBSP in this study. For ease of representation, we use the notations $\delta^-(i)$ and $\delta^+(i)$ to represent arcs $(i, j) \in A$ that end and start at node $i$, respectively. The decision variable is defined as follow:

- $x_{ij}^k$: binary variable, is set to 1 if an EB of type $k \in K$ is assigned to operate on arc or indicator $(i, j) \in A \cup I$, and 0 otherwise.

The auxiliary variables are defined as follows:

- $y_i^k$: continuous variable, denotes the remaining battery power of an EB of type $k \in K$ after completing node $i \in D \cup T \cup F$.
- $s_{f_i}$: continuous variable, denotes the start time of charging node $f_i \in F$.
- $t_{f_i}$: continuous variable, denotes the charging duration of charging node $f_i \in F$.
- $u_{n_t f_i}$: binary variable, is set to one if the EB at charging node $f_i \in F$ is under charge at time node $n_t$.

The objective of the MIP can be formulated as Eq. (5):

$$\min z_1 + z_2 + z_3 + z_4 \tag{5}$$

$$z_1 = \sum_{k\in K}\sum_{(o,j)\in\delta^+(o)} c^k x^k_{oj} \tag{5.1}$$

$$z_2 = \sum_{k\in K}\sum_{(i,j)\in A, j\notin F\cup D} F_{DC}\left(\frac{y^k_j}{E^k}, \frac{y^k_i}{E^k}\right)x^k_{ij} + \sum_{k\in K}\sum_{i\in T}\left[F_{DC}\left(\frac{y^k_i - e^k_{if_i}}{E^k}, \frac{y^k_i}{E^k}\right) + F_{DC}\left(\frac{y^k_i - e^k_{if_i}}{E^k}, \frac{y^k_{f_i}}{E^k}\right)\right]x^k_{if_i} + \sum_{k\in K}\sum_{(i,d)\in\delta^-(d)}\left[F_{DC}\left(\frac{y^k_i - e^k_{id}}{E^k}, \frac{y^k_i}{E^k}\right) + F_{DC}\left(\frac{y^k_i - e^k_{id}}{E^k}, 1\right)\right]x^k_{id} \tag{5.2}$$

$$z_3 = \sum_{k\in K}\sum_{i\in T} c_e\left(y^k_{f_i} - y^k_i + e^k_{if_i}\right)x_{if_i} + \sum_{k\in K}\sum_{(i,d)\in\delta^-(d)} c_e\left(E^k - y^k_i + e^k_{id}\right)x^k_{id} \tag{5.3}$$

$$z_4 = \sum_{i\in T} c_t t_i + \sum_{k\in K}\sum_{(i,j)\in A} c_t t_{ij} x^k_{ij} \tag{5.4}$$

The objective is to minimize the total cost of planning and operational stages, including four components. The first component ($z_1$, Eq. 5.1) calculates the sum of the vehicle depreciation cost of all EBs, where $c^k$ is the daily depreciation cost of a single bus of type $k$ except for the battery cost. The second component ($z_2$, Eq. 5.2) calculates the battery degradation cost. The third component ($z_3$, Eq. 5.3) is the cost of electricity consumption from charging activities, including charging during operation and fully charging after finishing all tasks, where $c_e$ denotes the electricity cost per kWh. The fourth component ($z_4$, Eq. 5.4) is the time-dependent labor cost, where $c_t$ represents the labor cost per minute for service trips and deadhead trips.

The constraints of the MIP model can be formulated as follows:

$$\sum_{k\in K}\sum_{(i,j)\in\delta^-(j)} x^k_{ij} = 1 \quad \forall j \in T \tag{6}$$

$$\sum_{k\in K} x^k_{if_i} \le 1 \quad \forall i \in T \tag{7}$$

$$\sum_{(i,j)\in\delta^+(i)} x^k_{ij} - \sum_{(j,i)\in\delta^-(i)} x^k_{ji} = 0 \quad \forall k \in K,\ \forall i \in T \cup F \tag{8}$$

$$x^k_{if_i} - \sum_{(f_i,r)\in I} x^k_{f_i r} = 0 \quad \forall k \in K,\ \forall i \in T \tag{9}$$

$$\sum_{(o,j)\in\delta^+(o)} x^k_{oj} - \sum_{(i,d)\in\delta^-(d)} x^k_{id} = 0 \quad \forall k \in K \tag{10}$$

$$s_{f_i} = \sum_{k\in K}\sum_{(f_i,r)\in I} s_r x^k_{f_i r} \quad \forall f_i \in F \tag{11}$$

$$t_{f_i} = \sum_{k\in K}\sum_{(f_i,r)\in I} t_r x^k_{f_i r} \quad \forall f_i \in F \tag{12}$$

$$u_{n_t f_i} = \sum_{k\in K}\sum_{(f_i,r)\in I} u_{n_t r} x_{f_i r} \quad \forall n_t \in N_t,\ \forall f_i \in F \tag{13}$$

$$s_{f_i} + t_{f_i} + t_{f_i j} - M\left(1 - \sum_{k\in K} x^k_{f_i j}\right) \le s_j \quad \forall f_i \in F,\ \forall (f_i, j) \in A \tag{14}$$

$$y^k_i - e^k_j - e^k_{ij} + M\left(1 - \sum_{k\in K} x^k_{ij}\right) \ge y^k_j \quad \forall k \in K,\ \forall j \in T \cup \{d\},\ \forall (i,j) \in \delta^-(j) \tag{15}$$

$$y^k_i - e^k_j - e^k_{ij} - M\left(1 - \sum_{k\in K} x^k_{ij}\right) \le y^k_j \quad \forall k \in K,\ \forall j \in T \cup \{d\},\ \forall (i,j) \in \delta^-(j) \tag{16}$$

$$F_{NC}\left(\frac{y^k_i - e^k_{if_i}}{E^k},\ t_{f_i}\right) + M\left(1 - \sum_{k\in K} x^k_{if_i}\right) \ge y^k_{f_i} \quad \forall k \in K,\ \forall i \in T \tag{17}$$

$$F_{NC}\left(\frac{y_i^k - e_{if_i}^k}{E^k},\ t_{f_i}\right) - M\left(1 - \sum_{k\in K} x_{if_i}^k\right) \le y_{f_i}^k \quad \forall k \in K,\ \forall i \in T \tag{18}$$

$$y_o^k = E^k \quad \forall k \in K \tag{19}$$

$$\sigma E^k \le y_i^k \le E^k \quad \forall k \in K, \forall i \in D \cup T \cup F \tag{20}$$

$$\sum_{k\in K}\sum_{i\in T} u_{n_t f_i} x_{if_i}^k \le C \quad \forall n_t \in N_t \tag{21}$$

Constraint (6) ensures that every service trip is fulfilled exactly once. Constraint (7) ensures that every possible charging event can be performed at most once. Constraint (8) represents flow conservation. Constraint (9) requires that every charging event is assigned to a virtual charging node. Constraint (10) enforces that the numbers of multi-type buses departing from and returning to the depot are the same. Constraints (11) to (13) ensure that the start time, duration, and occupation of a charging node are consistent with the assigned virtual charging node. Constraint (14) specifies the time compatibility of the connection between charging nodes and their subsequent trip nodes, where $M$ is a sufficiently large number. Constraints (15) to (18) specify the energy compatibility of the connection between nodes and their subsequent nodes when $x_{ij}^k$ equals 1, where $M$ is a sufficiently large number. Constraint (19) ensures that buses are fully charged when departing from the depot and starting their daily operation. Constraint (20) ensures the remaining battery power of the EBs at any time node within a reasonable range, where $\sigma$ is the battery safety level during operation. Constraint (21) guarantees that the total number of EBs under charging at any time node does not exceed the charging station capacity, where $C$ denotes the charging station capacity (in other words, the number of usable charging plugs in the station).

## 3. Solution algorithm

As the EBSP is an NP-hard problem (Li, 2014), to solve the model with a large number of variables within a reasonable time, we adopt the Adaptive Large Neighborhood Search (ALNS) algorithm. The ALNS has been widely applied to various vehicle routing problems, vehicle scheduling problems, and other related extensions (Azi et al., 2014; Demir et al., 2012; Kovacs et al., 2012; Mattos Ribeiro and Laporte, 2012; Ropke and Pisinger, 2006; Sacramento et al., 2019; Wen et al., 2016). Since the trip nodes in EBSP are similar to the customers with time windows in VRP, the ALNS can be used to solve the EBSP and has been proven its efficiency (Wen et al., 2016).

The ALNS explores a large neighborhood of the solution by destroying and repairing the current solution to increase the searching range and the likelihood of obtaining better solutions. A destroy operator disrupts part of the current solution while a repair operator rebuilds the destroyed solution. ALNS uses multiple destroy and repair operators and dynamically selects a pair of operators in each iteration according to their weights, which are adaptively adjusted based on the performance of each operator in previous iterations. The repaired solution is accepted based on a predefined criterion, and the algorithm stops when the stop criterion is met.

The framework of our ALNS is illustrated in Algorithm 1. The solution is a schedule, consisting of trip chains to be completed by EBs. In a trip chain, an EB of type $k$ departs from depot $o$ and returns to depot $d$, and is assigned to complete a series of trip nodes, as well as charging nodes if necessary. A sample schedule with 15 trip nodes and 4 trip chains is shown in Fig. 3. The initial solution is

**Algorithm 1:** Pseudocode of ALNS.

| Steps | Process |
|---|---|
| 1 | **initialize** a feasible solution $x_0$ |
| 2 | $x^* = x_0$; $x = x_0$ |
| 3 | $T = T_0$ |
| 4 | **repeat**: |
| 5 | $\eta$ = select a random number between $\eta_{max}$ and $\eta_{min}$ for operators |
| 6 | Choose a destroy operator and a repair operator based on their weights |
| 7 | $x'$ = the resulting solution after applying the destroy and repair operators to $x$ |
| 8 | Check the feasibility of $x'$ and add penalty cost if infeasible |
| 9 | **if** $x'$ is feasible and $f(x') < f(x^*)$: |
| 10 | $x^* = x_0$; $x = x'$ |
| 11 | **else if** $f(x') < f(x)$: |
| 12 | $x = x'$ |
| 13 | **else if** $e^{(f(x^*)-f(x'))/T}$ < random (0,1): |
| 14 | $x = x'$ |
| 15 | adjust weights of destroy and repair operators based on the performance of $x'$ |
| 16 | $T = \epsilon T$ |
| 17 | **if** $x^*$ doesn't change in $Iter_{uc}$ iterations: |
| 18 | **break** |
| 19 | **until** iteration $Iter_{max}$ is reached |
| 20 | **return** $x^*$ |

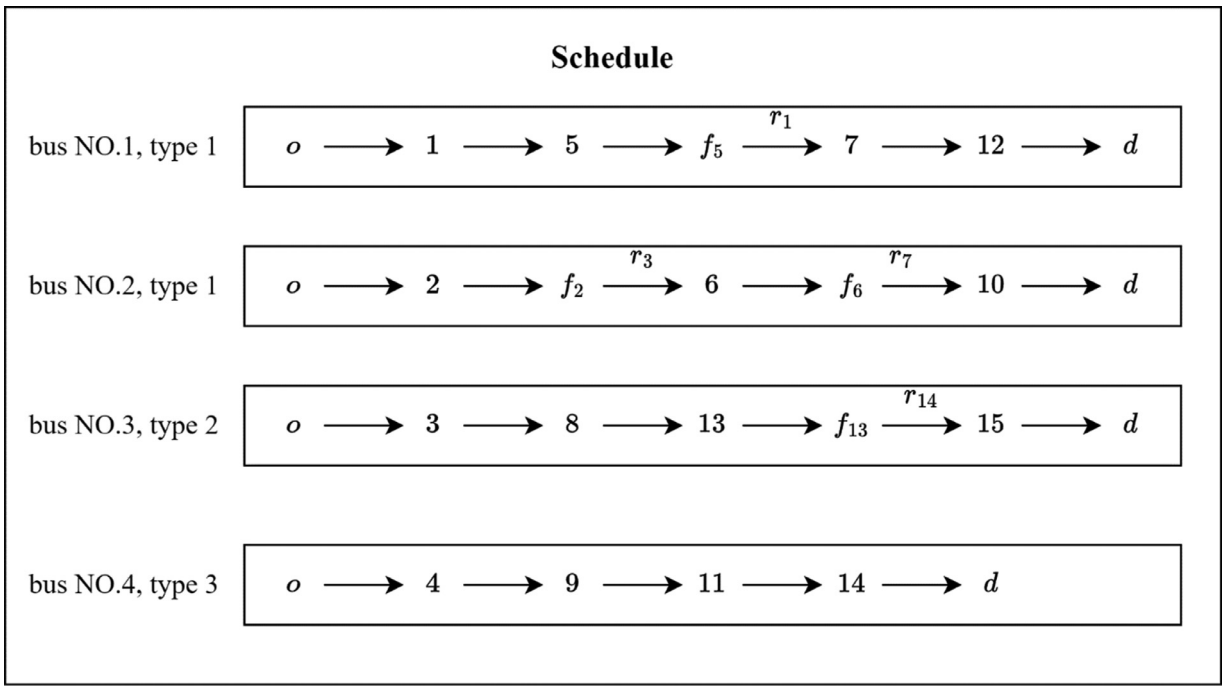


**Fig. 3.** A sample EBs schedule.

obtained by a greedy heuristic. The trip nodes are sorted in ascending order of their start time and iteratively added to the solution. We insert each node to the end of a trip chain in the solution that leads to the minimum increase of the objective function. When a trip node cannot be completed by the current EBs in the solution, we add a new bus of random type $k$ to the solution to fulfill the trip node. A roulette wheel selection and an adaptive weight adjustment method proposed by Ropke and Pisinger (2006) are employed for operator selection. After destroying and repairing the solution, the feasibility of the solution is checked and a penalty cost is added to the solution if it is infeasible. The ALNS stops when a predefined maximum iteration $Iter_{max}$ is reached or the best solution does not improve within $Iter_{uc}$ iterations. In each iteration, if the new solution $x'$ is better than the best solution $x^*$ and is feasible, it is accepted as the best solution. Else, if the new solution is better than the current solution $x$, it is also accepted and updated as the current solution, but if the new solution is no better than the current one, it is accepted by a probability $e^{(f(x^*)-f(x'))/T}$, in which function $f$ calculates the operating cost of solution $x$, and $T$ is the temperature same as the one in simulated annealing. Temperature $T$ is initialized by $T_0$ and decreases over iterations, making ALNS more likely to reject poor solutions towards the end.

In order to further optimize the fleet composition, when the iteration reaches $iter_{ds}$, the number of trips to remove in the trip chains fulfilled by vehicle type $k \in K$ is specified. Let $\psi_k$ be the proportion of removed trips belonging to vehicle type $k$ in the removed trips and $\sum_{k\in K} \psi_k = 1$. In each iteration, the number of removed trips of type $k$ is $\lfloor \psi_k \eta + 0.5 \rfloor$ and the $\psi_k$ of bus type $k$ with a larger driving range and higher investment increases by a constant rate $\Omega$.

The destroy operators, the repair operators, and the penalty are described in Appendix B. The designed algorithm demonstrates convergence of the optimized result, as shown in Appendix B.

## 4. Case studies

To investigate the robustness of the operational suggestions under traffic uncertainty, operation data of bus line 4, including travel time and energy consumption of each trip service in Nanjing, is expanded to a real-world multi-line network (Lines 4, 52, and 99), which has similar traffic conditions and line lengths. A case study based on the empirical single-depot multi-line bus network in Nanjing is conducted. Section 4.1 describes the information about this bus system in detail. Section 4.2 introduces the method to generate random samples of the bus network using empirical operational data of a single bus line to simulate the uncertainty of trip travel time and energy consumption. In the case study, a sensitive analysis of charging station capacity is conducted, and the charging station capacity $C$ is set in the range from 2 to 20 with an interval of 2. In each scenario, 30 timetables, generated using the method in Section 4.2, are optimized to simulate the uncertain travel time and energy consumption. In Section 4.3, we analyze and discuss the cost-effectiveness and robustness of the optimization results from the perspectives of cost and fleet compositions in the planning stage. Section 4.4 further discusses the results of the partial charging schedule and proposes suggestions for charging strategy for the operational stage. The power demand of the charging station and its impact on the power grid are further discussed in Section 4.5. Note that for the study case, Time-of-Use (TOU) electricity price is not adopted according to the real-world operation.


**Fig. 4.** The single-depot three-line bus network.

**Table 3**
EB types information.

| EBs type index | Battery capacity (kWh) | Cost (CNY) |
|---|---|---|
| A | 100 | 2260000 |
| B | 170 | 2548500 |
| C | 256 | 2918000 |

### *4.1. Bus system profile*

The bus system information includes details about the single-depot multi-line bus network, information on EBs, and cost data. Firstly, as shown in Fig. 4, the multi-line network (Line 4, 52, 99) shares the same depot, terminal, and charging station, which is located at the terminal. The districts of the selected three lines are located at the center of the urban area of Nanjing, China, where uncertainties about the trip duration and energy consumption are pronounced due to extremely congested road traffic and a high level of ridership. The round-trip mileages of Line 4, 52, and 99 are 24.8 km, 25.8 km, and 25.4 km respectively. The timetable for the network contains a total number of 275 round trips per day. The charging station, where EBs can park and get charged during operation, is equipped with 20 60 kW chargers. The depot, 10 km away from the terminal, provides parking and full charging at night for EBs. The operation hours of each day are from 5:00 am to 12:00 am, and the time interval $\beta$ for the time nodes set is 10 minutes.

Secondly, we consider three types of EB Skywell NJL6100EV (H10 series) with different battery capacities and costs, shown in Table 3 (Skywell, 2023). The daily depreciation cost is calculated assuming an average lifetime of 12 years per EBs and 360 days of operation annually (Chicago Transit Authority, 2023). The battery price is calculated based on the average cost of a lithium-ion battery, which is $138 per kWh (Lawn Love, 2023). The energy consumption growth rate from Ji et al. (2022) is used to adjust the energy consumption for different EB types (Ji et al., 2022). The safety level SoC $\sigma$ is 20 %. The piecewise nonlinear charging function of the three EB types is illustrated in Fig. 5, with the breakpoints summarized in Table 4. The battery gets charged at a constant charging rate at full power until SoC reaches 80 %, after which charging rate drops concavely with lower power (H. Hõimoja et al., 2012).

Lastly, the electricity price for charging EBs in Nanjing is 0.6416 CNY per kWh and the average salary of a bus driver is 5500 CNY per month, which is 0.5 CNY per min assuming 22 working days per month and 8 hours per day.

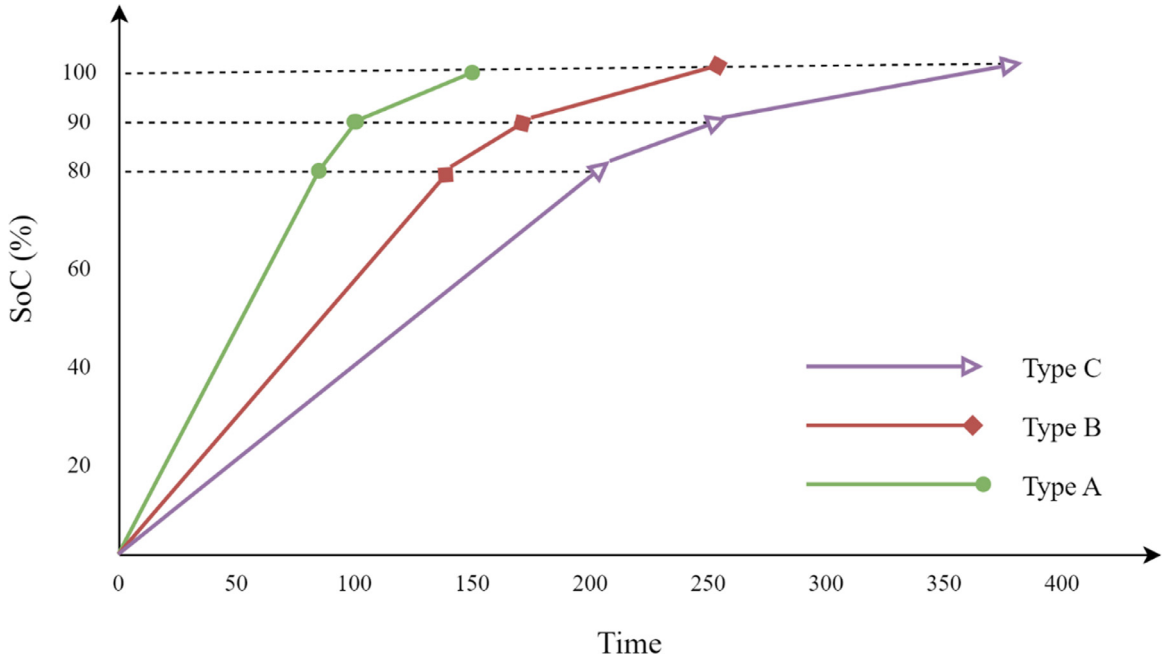


**Fig. 5.** Illustration of the nonlinear charging function of three EB types.

**Table 4**
Breakpoints of the piecewise nonlinear charging function.

| Breakpoint index | SoC (%) | Charging time (min) | | |
|---|---|---|---|---|
| | | Type A | Type B | Type C |
| 1 | 0 | 0 | 0 | 0 |
| 2 | 80 | 80 | 136 | 206 |
| 3 | 90 | 100 | 170 | 258 |
| 4 | 100 | 150 | 255 | 387 |

### *4.2. Random sample generation method*

To explore the influence of trip travel time and energy consumption variation on the decision robustness, we adopt a distribution simulation method proposed by Chen et al. to generate 30 random samples from the empirical operation data of bus Line 4, each containing a full-day timetable of the single-depot multi-line network mentioned above (Chen et al., 2023). To distinguish trips from different periods of a day, the K-Means method is used to cluster the trips into three groups, namely Peak, Off-Peak, and Morning/Evening (M/E), according to the historical trip travel time from AMAP API (AMP, 2023). The boxplots in Fig. 6 show the average level and variation of trip travel time and energy consumption of our real operational data of bus Line 4 in Nanjing. The period indexes (Peak, Off-Peak, M/E) are marked on each trip of the timetable before the simulation. The steps of the simulation method are shown in Fig. 7 and explained as follows:

(1) Choose a trip from the timetable in order and select the distribution of trip travel time and energy consumption, which are derived from the real-world data of Line 4;
(2) Randomly select a trip travel time and energy consumption based on the distribution;
(3) Scale them according to the distance of three bus lines;
(4) Fill the travel time and energy consumption back in the timetable;
(5) Iterate until all the trips have been filled.

### *4.3. Analysis of fleet cost-effectiveness and robustness*

Fig. 8 presents the average cost and cost composition of 30 timetables under different charging station capacities. The total cost is mainly composed of vehicle depreciation cost (on average 41.76 %) and battery degradation cost (on average 20.61 %), where the large proportion of battery degradation cost indicates that the battery degradation effect is not negligible and should be integrated into the scheduling problem. The electricity cost accounts for the smallest portion, with an average of 8.67 %. The electricity and labor cost stay stable as charging station capacity increases. However, an increasing charging station capacity leads to a decreasing vehicle

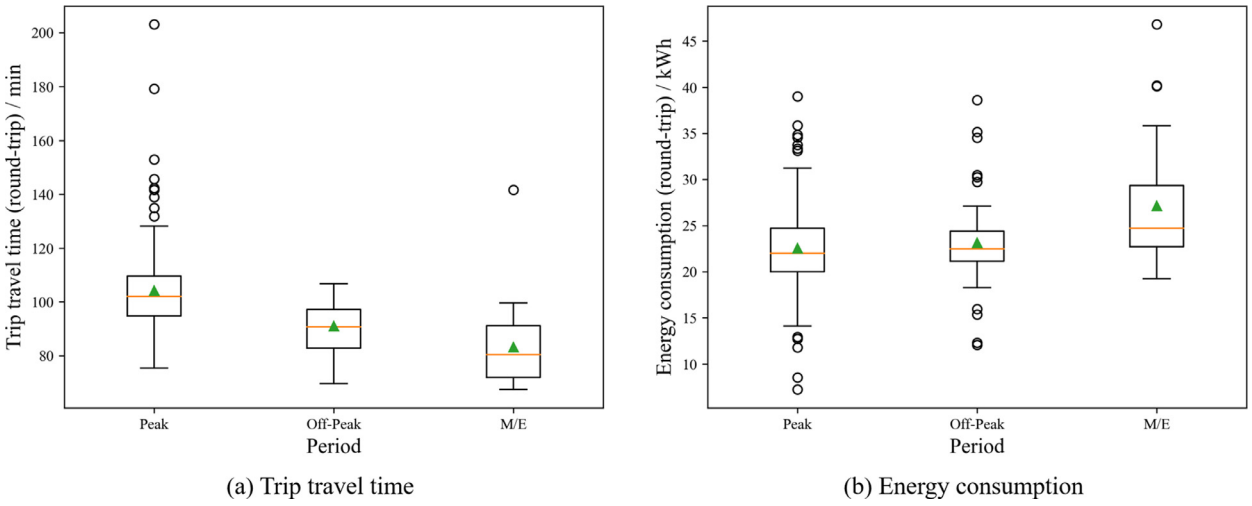


**Fig. 6.** Trip data description in Peak, Off-Peak, and M/E periods.

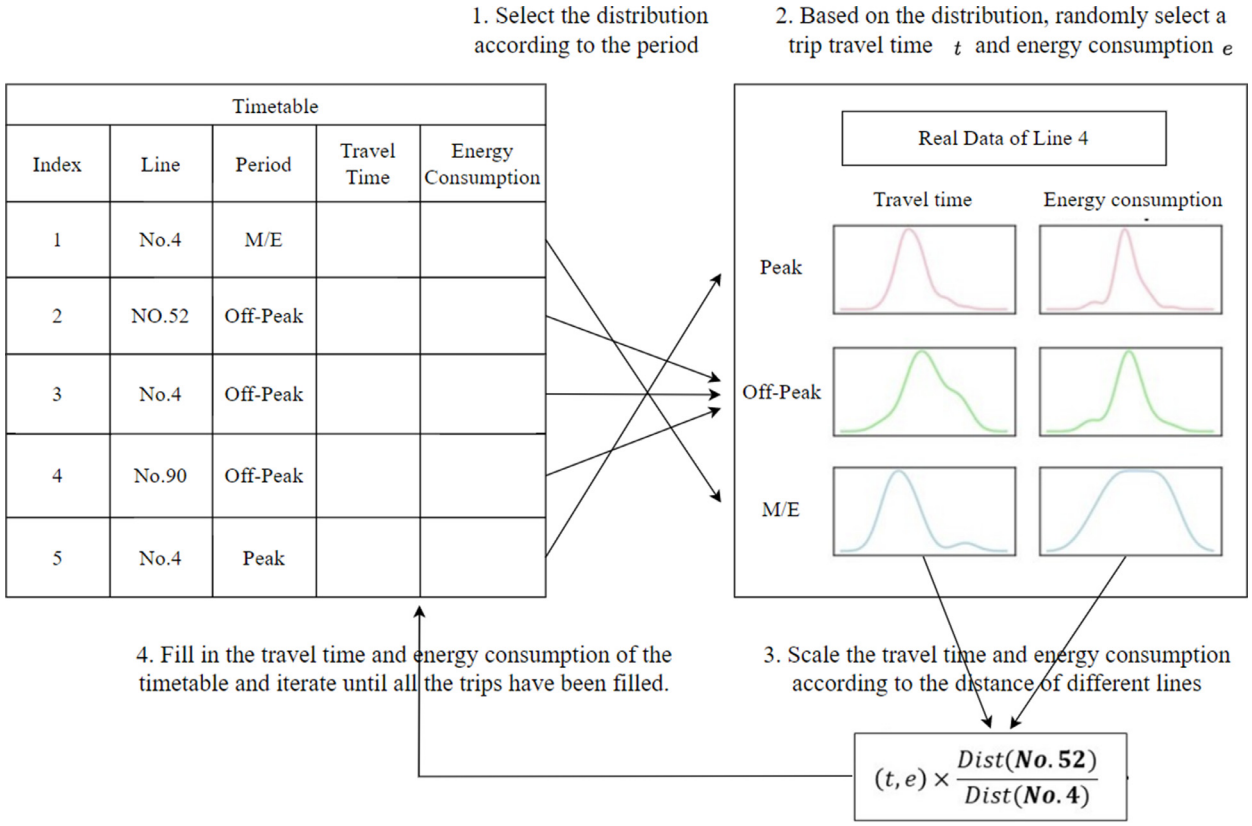


**Fig. 7.** The detailed steps of the distribution simulation method.

depreciation cost and battery degradation cost since more chargers increase the charging times during operation, which reduces the depth of charge for EBs. The need for EBs with larger battery capacity is also reduced at the same time. All cost components stabilize when the charging station capacity reaches eight. Considering the trend of total cost with regard to the station capacity, at least eight charging plugs in the station should be ensured for the cost-effectiveness of the studied bus network.

The average number of three EB types under different charging station capacities is shown in Fig. 9. The total number of EBs in the fleet varies slightly as charging station capacity increases, but when charging station capacity increases from two to eight, the proportion of type A (with the smallest battery capacity) increases, which results in a decreased vehicle depreciation cost. Although

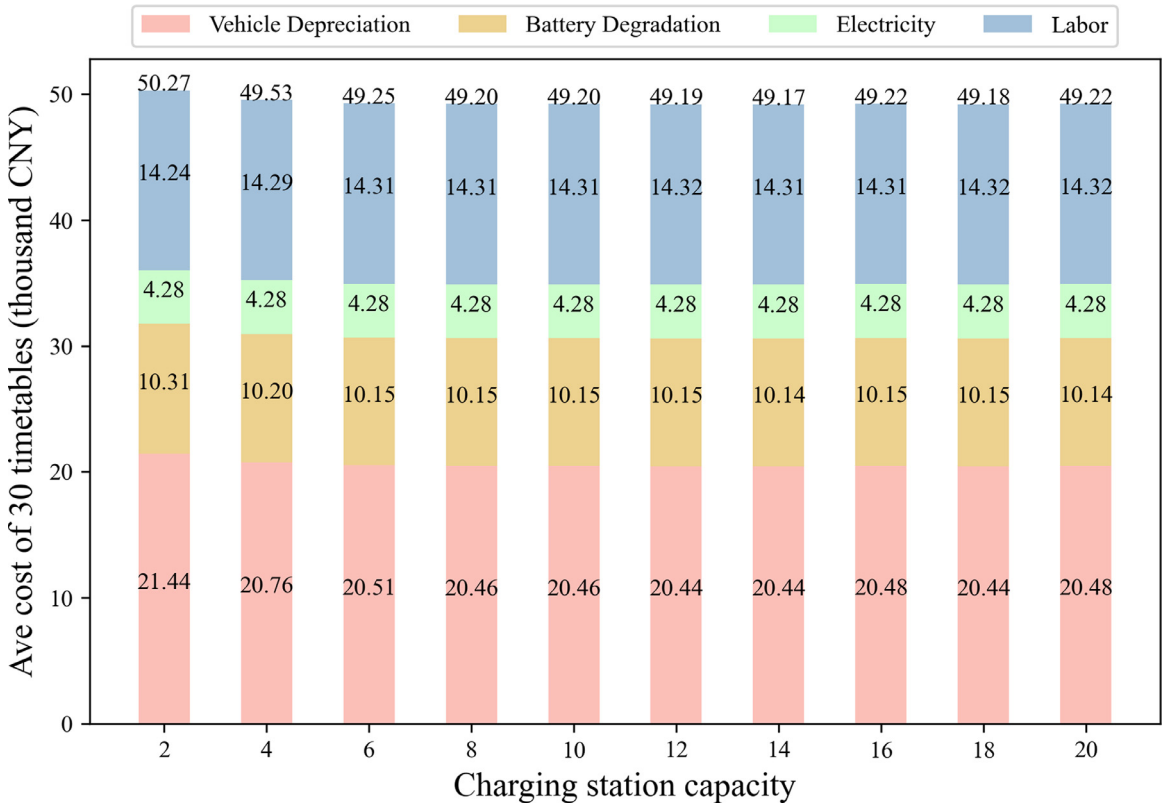


**Fig. 8.** Stack bar plot of average cost of four cost components and total cost in different charging station capacities.

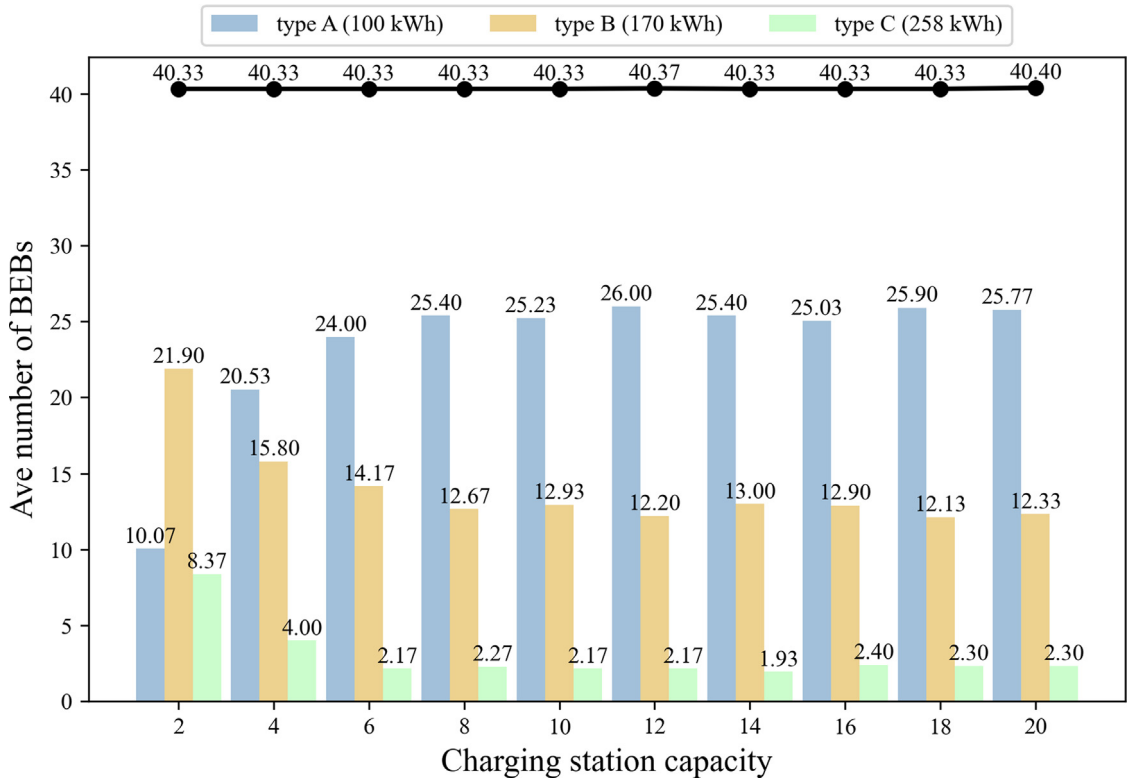


**Fig. 9.** Average number of three bus types needed in different charging station capacities.

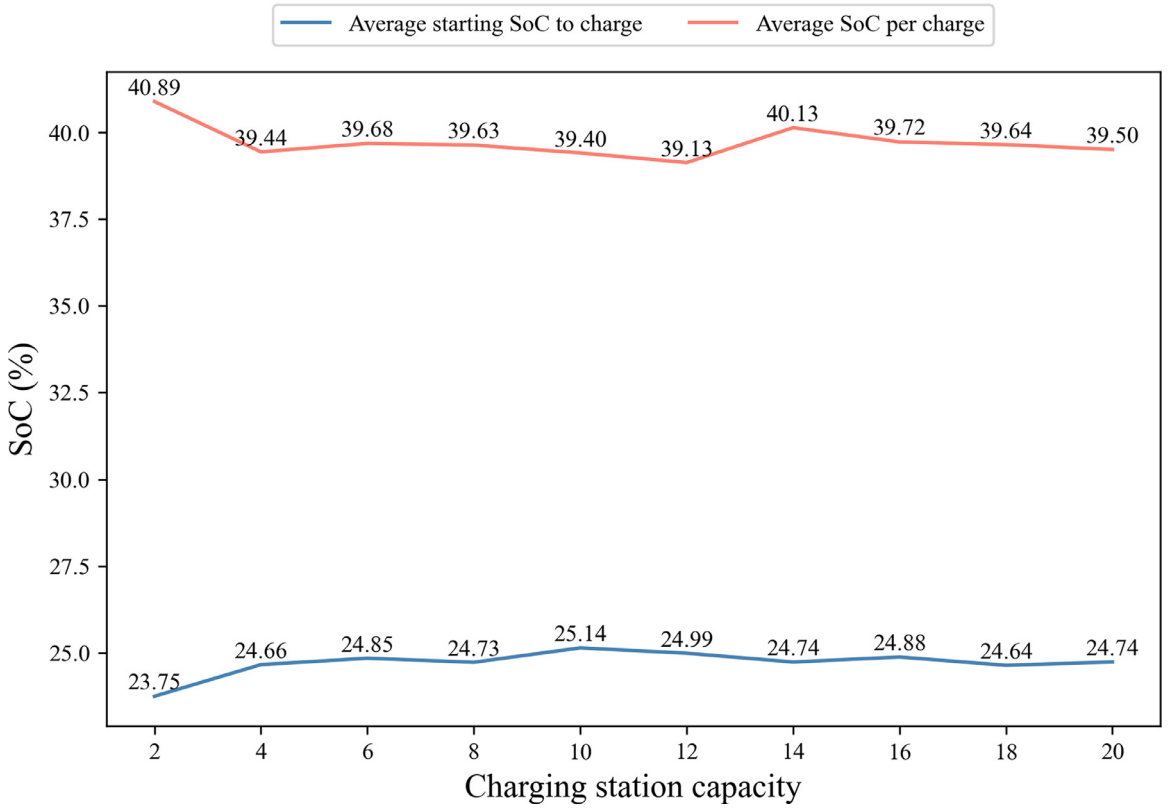


**Fig. 10.** Average starting SoC to charge and Average SoC per charge (including night charge).

the average total number of EBs has merely changed, the fleet composition varies with the expanding charging station capacity, which can be observed by the change in bus type share. For example, when the capacity equals two, type B and type C buses account for 75 % of the fleet. When the capacity increases to four, the share of type A significantly grows to 50.1 %. It can be observed that the fleet composition also keeps stable when the capacity is more than eight, consistent with the trend of the cost. Generally, both Fig. 8 and Fig. 9 indicate that the EB fleet decision remains stable, considering the uncertainty of travel time and energy consumption, when capacity reaches a certain threshold (which is eight in the studied case).

The increasing share of EBs with small battery capacity is due to the cost consideration of this problem set. According to Fig. 8, costs influenced by charging resources are mainly related to fleet composition and battery degradation. When sufficient charging resources (or charging capacity of the station) are provided, EBs have higher flexibility in determining the charging timeslots and durations. In this case, EBs with a smaller battery capacity are able to handle trips that were previously reserved for EBs with larger batteries. Additionally, more charging opportunities may lead to a decrease in the depth of discharge as well as the SoC per charge, which are shown in Fig. 10. This can lead to reduced battery degradation, as indicated above in Fig. 8. It should be noted that the cost-effectiveness result works for the proposed real-world case study and may vary depending on the parameter settings of different cases.

Fig. 11 and Fig. 12 show, respectively, the standard deviation of the cost and the number of EBs over different charging station capacities. The standard deviation of the optimized result is closely related to the resilience of the optimization decision to uncertain traffic conditions. A lower standard deviation indicates a higher resilience. From the perspective of cost (Fig. 11), the standard deviations of total cost and vehicle depreciation cost fluctuate. When the capacity is eight and twelve, the variations are comparably small, while from the perspective of the fleet (Fig. 12), the capacity of twelve illustrates a lower variation among different samples, indicating a robust condition. Fig. 12 also suggests that the number of type B and type C in the fleet is stable when the charging station capacity exceeds eight, and the minimum standard deviation of the fleet composition occurs at the charging station capacity twelve with the consideration of type A. Therefore, the highest resilience of the EB fleet to uncertain traffic conditions is demonstrated when the charging station capacity is twelve. Considering decision robustness, the fleet consisting of 26 EBs of type A, 13 EBs of type B, and 3 EBs of type C under the optimal charging station capacity 12 is the most economical choice. The average total cost is 49,192 CNY. The depot of the studied case is currently equipped with 20 chargers and the additional 8 chargers thus can be open to the public, as has been practiced in Shenzhen, China (Shenzhen Press Group Greater Bay Area News, 2023).

It should be noted that the operation uncertainty of EBs depends not only on the traffic condition uncertainties captured in this study, but also on other factors related to the passenger demand and the energy efficiency of the battery. The varied passenger

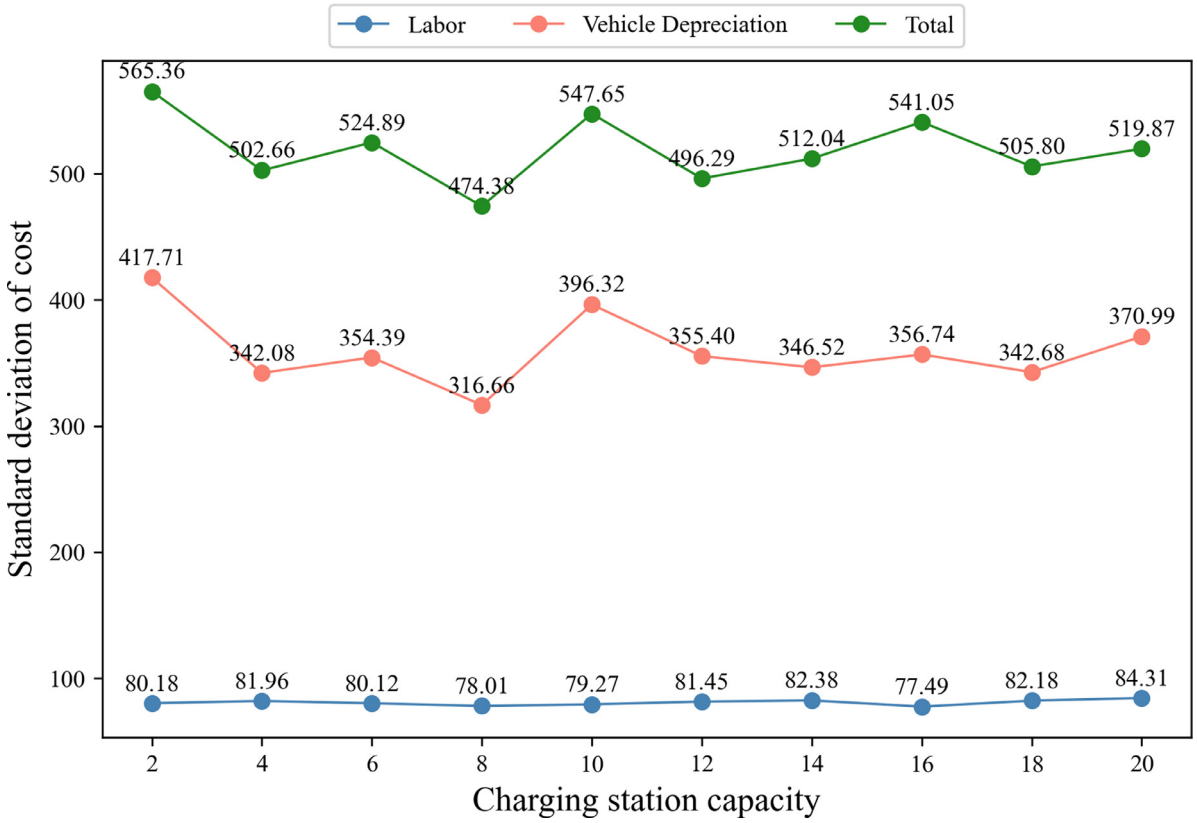


**Fig. 11.** Standard deviation of different costs in different charging station capacity.

demand at different stops on the route affects the weight of the bus, which further leads to varied energy consumption characteristics. In addition, the changed dwelling time also influences the actual operation of the bus, and the adjustment of the slack time should be included. For battery efficiency influenced by meteorological conditions, it's suggested that effective battery capacity and trip energy consumption of different temperature conditions should be pre-estimated for the schedule of different seasons.

### *4.4. Analysis of the optimized partial charging schedule*

In order to obtain operational suggestions from the optimized partial charging schedule, we analyze the charging times at different charging durations when the charging station capacity is twelve, as shown in Fig. 13. Notably, it can be observed that charging times and charging duration are negatively correlated. In the optimized partial charging schedule, 10-minute charging is the most popular choice, and most charging sessions last no more than 40 minutes, with few choices of longer charging durations. This indicates that the long charging duration should be avoided during operation.

The charging time count distribution over different charging durations and starting SoC ranges to charge at different periods of a day is presented in Fig. 14. The analysis is conducted under the optimal charging capacity (12). In the peak period, short-duration charging (10 and 20 minutes) is chosen more frequently, especially for the starting SoC between 20 % and 40 %. When the starting SoC is in the range between 20 % and 30 %, the choice of charging duration largely depends on the energy consumption of the next trip due to the energy constraints. In this scenario, 20-minute charging activities are preferred the most over 10-minute charging. In addition, 10-minute charging activities are also frequently selected when the starting SoC ranges from 40 % to 80 %, while in this SoC range, longer-duration charging is less preferred. These findings indicate that in the peak period when intensive trips occur, operators can prioritize the completion of trips, and 10-30 minutes of charging can be performed to recharge EBs. When the SoC range ranges from 50 % to 80 %, EBs can be charged for a shorter duration if the time constraint can be met before serving the next trips.

The charging time count for the off-peak period is quite similar to that in the peak period. However, the overall charging times in the off-peak period are about half of that in the peak period, due to fewer trips and charging demand being lower than that in the peak period. In the M/E period, charging times are rare, and most EBs choose to get 10-minute charging when their SoC is between 60 % and 80 %. The charges in M/E mainly happen in the morning period, which is followed by the peak period. Therefore, operators can choose to charge the EBs for a shorter duration after finishing their morning trips to ensure a safer and more robust SoC before the peak period.

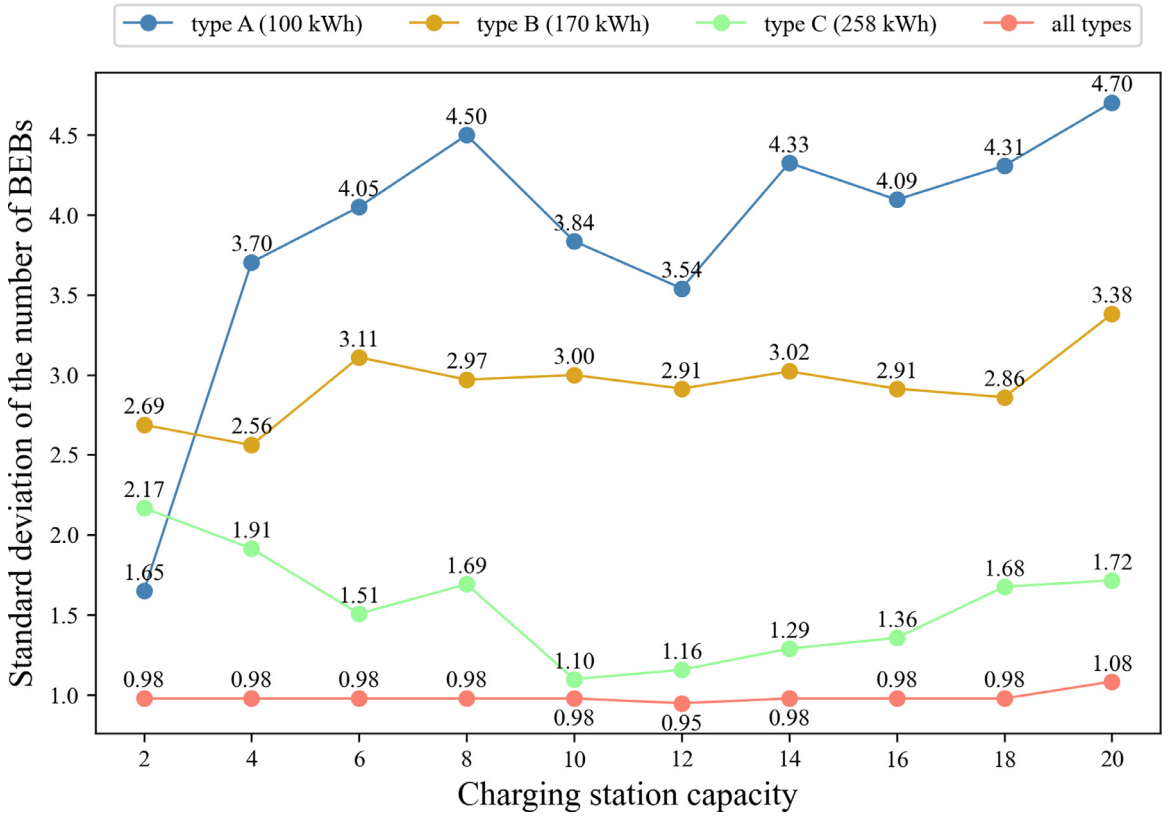


**Fig. 12.** Standard deviation of the number of EBs in different charging station capacity.

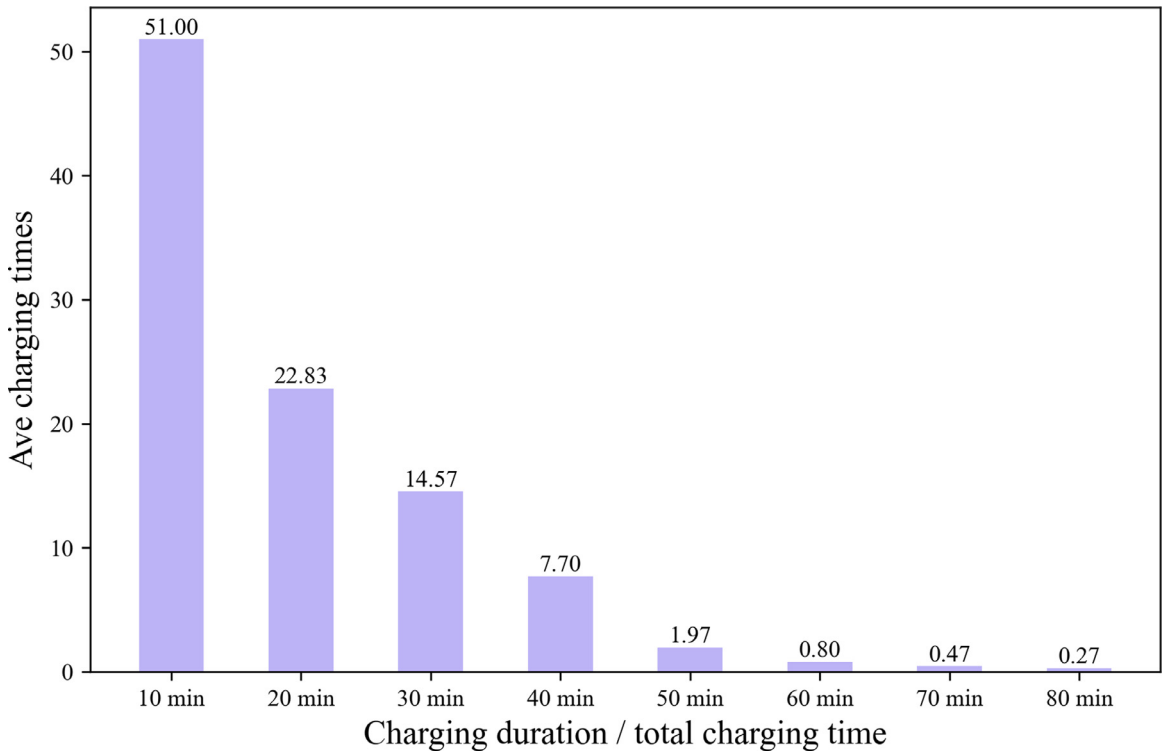


**Fig. 13.** Average charging times over charging duration and average total charging time when capacity is 12.

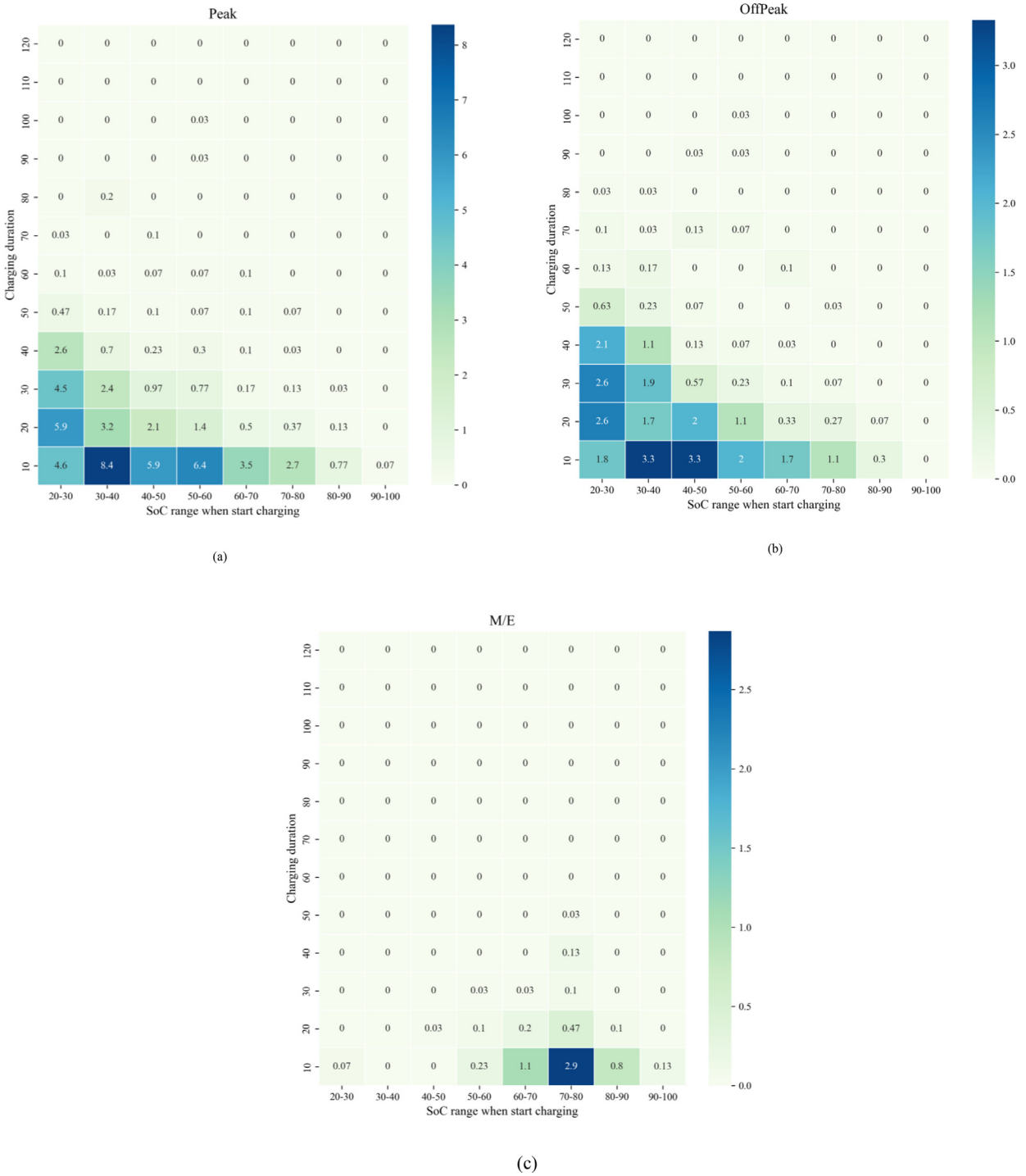


**Fig. 14.** Heat map of the average charging times in different charging duration and the starting SoC range of charging in three periods (Peak, Off-Peak, M/E). (a) The charging time count for different starting SoC of charging in the peak period; (b) The charging time count for different starting SoC of charging in the off-peak period; (c) The charging time count for different starting SoC of charging in the M/E period.

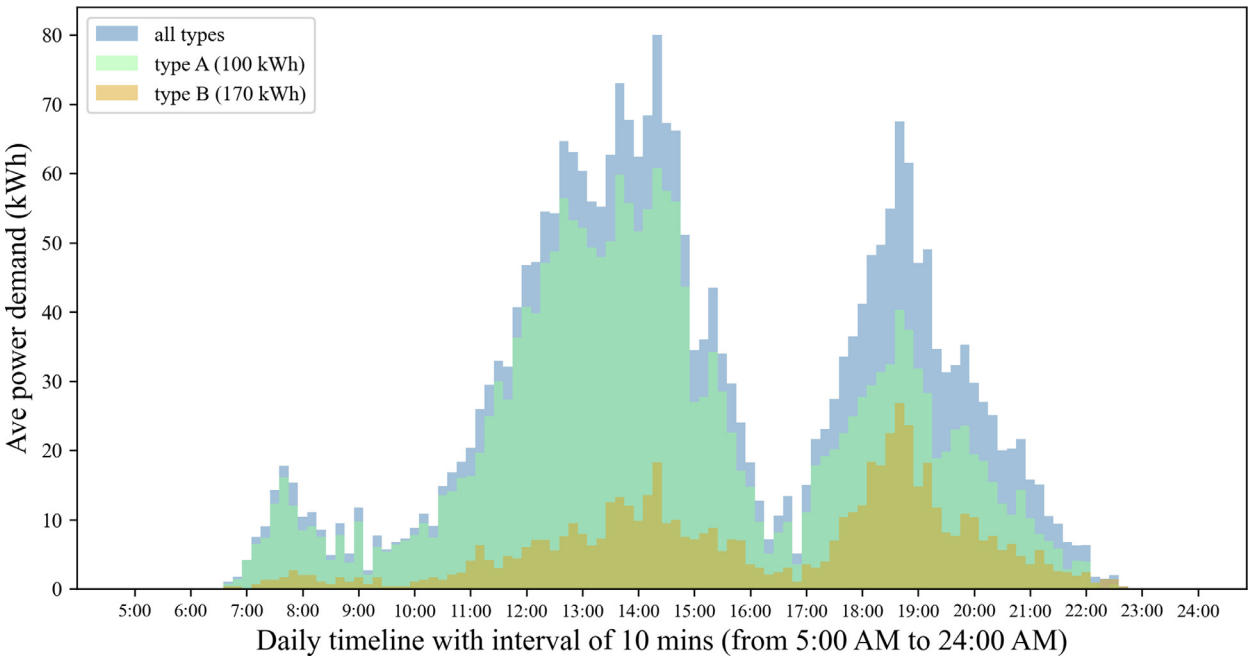


**Fig. 15.** Power demand distribution of the charging station over the operation time.

### *4.5. Analysis of the power demand in the charging station*

In order to investigate the impact of the charging schedule on the power grid, the power demand distribution of the charging station over the operation time when capacity is 12 is plotted in Fig. 15. The power demand distribution over a day in Jiangsu Province (where the studied case locates) is used as the control group, shown in Appendix C. Fig. 15 shows that the power peak and off-peak of different bus types occur at the same time periods, and the power demand of type A is much higher than that of type B, which is consistent with the fleet composition and the fact that EBs with smaller battery capacity require more charging. The power peak hours of the charging station are distributed from 11:30 am to 3:30 pm and from 5:30 pm to 8:30 pm. While these peak hours avoid the morning power peak hours from 9:00 am to 11:00 am in Jiangsu province, they overlap with the existing afternoon and evening peak hours, potentially increasing the load on the power grid during peak hours.

The great fluctuation of the EB charging power demand can be a potential risk to the stability of the regional electricity grid. At the present stage, the lack of TOU electricity price in the study area may lead to the concentration of EBs charging time. After the implementation of TOU, the charging cost during operation can be affected by the charging schedule. If the charging demand of the charging schedule is concentrated in the peak hours, the charging cost will increase, ultimately leading to the increase of the objective function. Therefore, TOU can be one of the solutions to shift peak charging demand to off-peak periods, which can be incorporated in the future study. Besides, since the current power system has been included in the carbon trading market, under the condition of electricity marketization, carbon price becomes a major part of the electricity price. Therefore, more renewable energy with lower carbon emissions can be attracted to supply power for the public transit network, and more optical-storage charging stations can also be adopted, further reducing the peak power loads of the power grid (National Development and Reform Comission, 2021; National Energy Administration, 2021). The future exploration should focus on understanding how the electricity market influence EB charging activities and its impact on the total operational cost.

## 5. Conclusion

In this study, we propose a time-expanded network to represent the bus-to-trip assignment and partial-charging schedule. Based on this network, an EBs scheduling problem considering multi-vehicle types, charging station capacity, nonlinear charging, and battery degradation is formulated as a mixed-integer programming (MIP) model. An adaptive large neighborhood search (ALNS) is developed to solve the problem. To simulate the uncertain conditions of the daily EB operation, distribution simulation is used to generate sampled trip timetables for robust suggestions on the charging schedule and resource assignment. A case study is conducted using the optimization algorithm and the simulation method to investigate the resource allocations of the EB fleet under different charging station capacities. Operational suggestions are derived from the optimized charging schedule.

In the resource planning stage, the study shows that a larger charging station capacity can reduce the total cost, but the total cost stays stable when the capacity exceeds a certain level. An increasing proportion of EBs with a smaller battery capacity due to sufficient charging duration is one of the major contributions to the reduced cost. Considering the decision robustness, which is reflected by

the standard deviation of cost and fleet composition, 12 charging plugs are the most cost-effective solution, and operators can thus open the rest chargers at the station to the public to get more revenue.

Under the optimal charging station capacity (which is 12 in our case), we further analyze the charging times distribution over different charging durations and starting SoC levels. The result shows that charging times decreases with the increasing charging duration, and EBs rarely charge for more than 50 minutes. In terms of different periods of a day, charging activities of 20-30 minutes are more recommended for EBs with a SoC lower than 30 % compared to the 10-minute duration to meet the energy constraint, especially in the peak and off-peak periods, while 10-minute charging activities are more favorable when SoC is between 30 % and 70 %. In the M/E period, operators can charge the EBs for 10 minutes when they finish their first trips in the morning in order to store sufficient energy for the peak period. Finally, the impact of the charging schedule on the power grid is analyzed, and the result reveals that the power peak hours of the charging schedule overlap with the power peak hours of the studied area, calling for the need for bus-grid coordination and effective guidance to shift the peak induced from charging activities.

The result analysis of this study can serve as a reference for vehicle and charging resource allocations, offering valuable charging suggestions during Peak, Off-Peak, and M/E periods. In future work, additional factors in the charging process, such as flexible charging power, micro-grid, and TOU electricity price, should be considered for a balanced grid power over time. Moreover, uncertainties besides traffic conditions, such as battery efficiencies and operation time reliability, need to be captured. As the battery degrades, the operation schedule needs to be re-optimized periodically with updated effective battery capacity to ensure its feasibility. Finally, to improve the model executability, algorithms with higher computational efficiency and accuracy should be developed to alleviate the complexity of larger-scale networks.

## Declaration of competing interest

The authors declare that they have no known competing financial interests or personal relationships that could have appeared to influence the work reported in this paper.

## CRediT authorship contribution statement

**Chenming Niu:** Conceptualization, Methodology, Software, Writing – original draft, Writing – review & editing. **Qiuzi Chen:** Methodology. **Ran Tu:** Conceptualization, Funding acquisition, Resources, Supervision, Writing – review & editing. **Di Huang:** Methodology, Writing – review & editing. **Yujian Ye:** Writing – review & editing.

## Acknowledgements

This study is funded by the Key Laboratory of Transport Industry of Comprehensive Transport Theory (Nanjing Modern Multimodal Transportation Laboratory (No. MTF2023006)), the National Natural Science Foundation of China (Nos. 52102409, 52207082), the Provincial Natural Science Foundation of Jiangsu Province (Nos. BK20210246, BK20220842), and the Provincial and Ministerial Key Laboratory Scientific Research Project (2242023K30017), Fundamental Research Funds for Central Universities (242023R4002); The Open Foundation of Key Laboratory of Transport Industry of Comprehensive Transport Theory. We thank Skywell Automobile, Nanjing, for supporting the bus data.

## Supplementary materials

Supplementary material associated with this article can be found, in the online version, at doi:10.1016/j.multra.2024.100165.

## References

Alvo, M., Angulo, G., Klapp, M.A., 2021. An exact solution approach for an electric bus dispatch problem. Transp. Res. E Logist. Transp. Rev. 156, 102528. doi:10.1016/j.tre.2021.102528.

AMP, 2023. AMAP API [WWW Document]. URL https://lbs.amap.com/api/webservice/guide/api/direction (accessed 5.30.23).

An, K., 2020. Battery electric bus infrastructure planning under demand uncertainty. Transp. Res. Part C Emerg. Technol. 111, 572–587. doi:10.1016/j.trc.2020.01.009.

Azi, N., Gendreau, M., Potvin, J.-Y., 2014. An adaptive large neighborhood search for a vehicle routing problem with multiple routes. Comput. Oper. Res. 41, 167–173. doi:10.1016/j.cor.2013.08.016.

Bao, Z., Li, J., Bai, X., Xie, C., Chen, Z., Xu, M., Shang, W.-L., Li, H., 2023. An optimal charging scheduling model and algorithm for electric buses. Appl. Energy 332, 120512. doi:10.1016/j.apenergy.2022.120512.

Barré, A., Deguilhem, B., Grolleau, S., Gérard, M., Suard, F., Riu, D., 2013. A review on lithium-ion battery ageing mechanisms and estimations for automotive applications. J. Power Sources 241, 680–689. doi:10.1016/j.jpowsour.2013.05.040.

Bie, Y., Ji, J., Wang, X., Qu, X., 2021. Optimization of electric bus scheduling considering stochastic volatilities in trip travel time and energy consumption. Comput. Aided Civ. Infrastruct. Eng. 36, 1530–1548. doi:10.1111/mice.12684.

Chen, Q., Niu, C., Tu, R., Li, T., Wang, A., He, D., 2023. Cost-effective electric bus resource assignment based on optimized charging and decision robustness. Transp. Res. D Transp. Environ. 118, 103724. doi:10.1016/j.trd.2023.103724.

Chicago Transit Authority, 2023. CTA Electric buses [WWW Document]. URL https://www.transitchicago.com/electricbus/.

Demir, E., Bektaş, T., Laporte, G., 2012. An adaptive large neighborhood search heuristic for the Pollution-Routing Problem. Eur. J. Oper. Res. 223, 346–359. doi:10.1016/j.ejor.2012.06.044.

Dunn, J.B., Gaines, L., Kelly, J.C., James, C., Gallagher, K.G., 2015. The significance of Li-ion batteries in electric vehicle life-cycle energy and emissions and recycling's role in its reduction. Energy Environ. Sci. 8, 158–168. doi:10.1039/C4EE03029J.

Guo, F., Zhang, J., Huang, Z., Huang, W., 2022. Simultaneous charging station location-routing problem for electric vehicles: Effect of nonlinear partial charging and battery degradation. Energy 250, 123724. doi:10.1016/j.energy.2022.123724.

Höimoja, H., Rufer, A., Dziechciaruk, G., Vezzini, A., 2012. An ultrafast EV charging station demonstrator. In: International Symposium on Power Electronics Power Electronics, Electrical Drives, Automation and Motion, Sorrento, Italy, pp. 1390–1395.
Han, Sekyung, Han, Soohee, Aki, H., 2014. A practical battery wear model for electric vehicle charging applications. Appl. Energy 113, 1100–1108. doi:10.1016/j.apenergy.2013.08.062.
He, Y., Liu, Z., Song, Z., 2022. Integrated charging infrastructure planning and charging scheduling for battery electric bus systems. Transp. Res. D Transp. Environ. 111, 103437. doi:10.1016/j.trd.2022.103437.
He, Y., Liu, Z., Song, Z., 2020. Optimal charging scheduling and management for a fast-charging battery electric bus system. Transp. Res. E Logist. Transp. Rev. 142, 102056. doi:10.1016/j.tre.2020.102056.
Ji, J., Bie, Y., Zeng, Z., Wang, L., 2022. Trip energy consumption estimation for electric buses. Commun. Transp. Res. 2, 100069. doi:10.1016/j.commtr.2022.100069.
Jiang, M., Zhang, Y., Zhang, Y., 2021. Optimal electric bus scheduling under travel time uncertainty: a robust model and solution method. J. Adv. Transp. 2021, 1–19. doi:10.1155/2021/1191443.
Kovacs, A.A., Parragh, S.N., Doerner, K.F., Hartl, R.F., 2012. Adaptive large neighborhood search for service technician routing and scheduling problems. J. Sched. 15, 579–600. doi:10.1007/s10951-011-0246-9.
Lam, L., Bauer, P., 2013. Practical capacity fading model for li-ion battery cells in electric vehicles. IEEE Trans. Power Electron. 28, 5910–5918. doi:10.1109/TPEL.2012.2235083.
Land Transport Authority, 2022. Land Transport Master Plan 2040. Singapore.
Lawn Love, 2023. How Much Does a Lithium-Ion Battery Cost in 2023? [WWW Document]. URL https://lawnlove.com/blog/lithium-ion-battery-cost/.
Leou, R.-C., Hung, J.-J., 2017. Optimal charging schedule planning and economic analysis for electric bus charging stations. Energies (Basel) 10, 483. doi:10.3390/en10040483.
Li, J.-Q., 2014. Transit bus scheduling with limited energy. Transp. Sci. 48, 521–539. doi:10.1287/trsc.2013.0468.
Li, L., Lo, H.K., Xiao, F., 2019. Mixed bus fleet scheduling under range and refueling constraints. Transp. Res. Part C Emerg. Technol. 104, 443–462. doi:10.1016/j.trc.2019.05.009.
Liu, K., Gao, H., Liang, Z., Zhao, M., Li, C., 2021. Optimal charging strategy for large-scale electric buses considering resource constraints. Transp. Res. D Transp. Environ. 99, 103009. doi:10.1016/j.trd.2021.103009.
Liu, Z., Song, Z., 2017. Robust planning of dynamic wireless charging infrastructure for battery electric buses. Transp. Res. Part C Emerg. Technol. 83, 77–103. doi:10.1016/j.trc.2017.07.013.
Manzolli, J.A., Trovão, J.P.F., Henggeler Antunes, C., 2022. Electric bus coordinated charging strategy considering V2G and battery degradation. Energy 254, 124252. doi:10.1016/j.energy.2022.124252.
Mattos Ribeiro, G., Laporte, G., 2012. An adaptive large neighborhood search heuristic for the cumulative capacitated vehicle routing problem. Comput. Oper. Res. 39, 728–735. doi:10.1016/j.cor.2011.05.005.
Montoya, A., Guéret, C., Mendoza, J.E., Villegas, J.G., 2017. The electric vehicle routing problem with nonlinear charging function. Transp. Res. Part B Methodol. 103, 87–110. doi:10.1016/j.trb.2017.02.004.
National Development and Reform Comission, 2021. Notice of the National Development and Reform Commission on Further improving the time-of-use Tariff Mechanism [WWW Document]. URL https://www.gov.cn/zhengce/zhengceku/2021-07/29/content_5628297.htm (accessed 5.29.23).
National Energy Administration, 2021. The multiple implications of TOU pricing policy.
Pelletier, S., Jabali, O., Laporte, G., Veneroni, M., 2017. Battery degradation and behaviour for electric vehicles: review and numerical analyses of several models. Transp. Res. Part B Methodol. 103, 158–187. doi:10.1016/j.trb.2017.01.020.
Pelletier, S., Jabali, O., Mendoza, J.E., Laporte, G., 2019. The electric bus fleet transition problem. Transp. Res. Part C Emerg. Technol. 109, 174–193. doi:10.1016/j.trc.2019.10.012.
Qin, N., Gusrialdi, A., Paul Brooker, R., T-Raissi, A., 2016. Numerical analysis of electric bus fast charging strategies for demand charge reduction. Transp. Res. Part A Policy Pract. 94, 386–396. doi:10.1016/j.tra.2016.09.014.
Quarles, N., Kockelman, K.M., Mohamed, M., 2020. Costs and benefits of electrifying and automating bus transit fleets. Sustainability 12, 3977. doi:10.3390/su12103977.
Rogge, M., van der Hurk, E., Larsen, A., Sauer, D.U., 2018. Electric bus fleet size and mix problem with optimization of charging infrastructure. Appl. Energy 211, 282–295. doi:10.1016/j.apenergy.2017.11.051.
Ropke, S., Pisinger, D., 2006. An adaptive large neighborhood search heuristic for the pickup and delivery problem with time windows. Transp. Sci. 40, 455–472. doi:10.1287/trsc.1050.0135.
Sacramento, D., Pisinger, D., Ropke, S., 2019. An adaptive large neighborhood search metaheuristic for the vehicle routing problem with drones. Transp. Res. Part C Emerg. Technol. 102, 289–315. doi:10.1016/j.trc.2019.02.018.
Shenzhen Press Group Greater Bay Area News, 2023. Shenzhen citizens can go to the bus station to charge new energy vehicles [WWW Document]. URL https://www.sznews.com/news/content/2023-03/07/content_30106225.htm.
Skywell, 2023. Skywell BEBs Page [WWW Document]. URL https://www.skywellcorp.com/index.php/product/detail/5.html.
Tang, X., Lin, X., He, F., 2019. Robust scheduling strategies of electric buses under stochastic traffic conditions. Transp. Res. Part C Emerg. Technol. 105, 163–182. doi:10.1016/j.trc.2019.05.032.
The State Council of People's Republic of China, 2021. Modern comprehensive transportation system for 14th Five-Year Plan [WWW Document]. URL http://www.gov.cn/zhengce/content/2022-01/18/content_5669049.htm.
Tu, R., Gai, Y.(Jessie), Farooq, B., Posen, D., Hatzopoulou, M., 2020. Electric vehicle charging optimization to minimize marginal greenhouse gas emissions from power generation. Appl. Energy 277. doi:10.1016/j.apenergy.2020.115517.
United States Department of Transportation, 2021. Fiscal Year 2021 Low or No-Emission (Low-No) Bus Program Projects [WWW Document]. URL https://www.transit.dot.gov/funding/grants/fiscal-year-2021-low-or-no-emission-low-no-bus-program-projects (accessed 5.30.23).
Wang, A., Tu, R., Gai, Y., Pereira, L.G., Vaughan, J., Posen, I.D., Miller, E.J., Hatzopoulou, M., 2020. Capturing uncertainty in emission estimates related to vehicle electrification and implications for metropolitan greenhouse gas emission inventories. Appl. Energy 265. doi:10.1016/j.apenergy.2020.114798.
Wang, Y., Huang, Y., Xu, J., Barclay, N., 2017. Optimal recharging scheduling for urban electric buses: A case study in Davis. Transp. Res. E Logist. Transp. Rev. 100, 115–132. doi:10.1016/j.tre.2017.01.001.
Wen, M., Linde, E., Ropke, S., Mirchandani, P., Larsen, A., 2016. An adaptive large neighborhood search heuristic for the Electric Vehicle Scheduling Problem. Comput. Oper. Res. 76, 73–83. doi:10.1016/j.cor.2016.06.013.
Wu, Z., Wang, M., Zheng, J., Sun, X., Zhao, M., Wang, X., 2018. Life cycle greenhouse gas emission reduction potential of battery electric vehicle. J. Clean. Prod. 190, 462–470. doi:10.1016/j.jclepro.2018.04.036.
Yıldırım, Ş., Yıldız, B., 2021. Electric bus fleet composition and scheduling. Transp. Res. Part C Emerg. Technol. 129, 103197. doi:10.1016/j.trc.2021.103197.
Zeng, Z., Wang, S., Qu, X., 2022. On the role of battery degradation in en-route charge scheduling for an electric bus system. Transp. Res. E Logist. Transp. Rev. 161, 102727. doi:10.1016/j.tre.2022.102727.
Zhang, L., Wang, S., Qu, X., 2021. Optimal electric bus fleet scheduling considering battery degradation and non-linear charging profile. Transp. Res. E Logist. Transp. Rev. 154, 102445. doi:10.1016/j.tre.2021.102445.
Zhang, Y., Xiong, R., He, H., Qu, X., Pecht, M., 2019. State of charge-dependent aging mechanisms in graphite/Li(NiCoAl)O2 cells: Capacity loss modeling and remaining useful life prediction. Appl. Energy 255, 113818. doi:10.1016/j.apenergy.2019.113818.
Zhou, Y., Meng, Q., Ong, G.P., 2022. Electric bus charging scheduling for a single public transport route considering nonlinear charging profile and battery degradation effect. Transp. Res. Part B Methodol. 159, 49–75. doi:10.1016/j.trb.2022.03.002.